CrossMark

Characteristics of precipitating monsoon clouds over rain-shadow and drought-hit regions of India using radar

S. B. Morwal[1] · S. G. Narkhedkar[1] · B. Padmakumari[1] · R. S. Maheskumar[1] · J. R. Kulkarni[1]

Abstract C-band radars were installed at Baramati and Shegaon as a part of operational cloud seeding program of Maharashtra State in the monsoon season (June–September) 2004. These provided first time a unique opportunity to study (1) characteristics of precipitating monsoon clouds (2) convection and (3) number of seedable clouds over Indian meteorological subdivisions of Madhya Maharashtra (rain-shadow) and Vidarbha (drought-hit). The monsoon season is divided into active and break periods. The cloud characteristics studied are: diurnal variation, cloud top heights and durations. Diurnal variation of cloud frequency shows maximum in the afternoon hours (10–11 UTC) and minimum in the early morning hours (3–4 UTC) in both the periods. Cloud tops show trimodal distributions with modes at 2–3, 8–9 and above 9 km. Mean cloud duration is 55 min. Congestus has been found prominent cloud type (65%) with mean top height of 6.76 km. Frequency of cumulonimbus clouds is found higher in the break periods. Cloud scale is taken as a metric for characterization of convection. Maximum frequency of cloud scale is found at C scale (mesoscale: area 100–1000 km^2). Mesoscale Convective System has been found dominating convection type. The convection over the area has been shown to be hybrid type, consisting of basic oceanic type modulated by land convection. Convective clouds having maximum reflectivities between 25 and 35 dBZ, suitable for hygroscopic and glaciogenic seeding, are found in a large number. Understanding of characteristics of clouds and convection is useful for the diagnostic and precipitation enhancement studies over the rain-shadow/drought-hit regions.

Keywords Characteristics of clouds and convection using radar · Rain-shadow region of Madhya Maharashtra · Drought-hit region of Vidarbha · Summer monsoon season · Active and break periods · Thermodynamical parameters · Large scale dynamical processes · Statistics of seedable convective clouds

1 Introduction

Mesoscale mountains entail the rain-shadow region on the lee side (Xie et al. 2006). Western Ghats (WG) are mesoscale mountains. These run parallel to west coast of India, in the north south direction at a distance of 50 km from the coast, with mean height of 0.9 km above mean sea level (amsl) and north–south length of 1100 km. A rain-shadow region is formed on the leeward side (east) of it with mean rainfall of 650 mm (Gunnell 1997). Figure 1a shows map of India and meteorological rain-shadow subdivisions. These are: (1) Madhya Maharashtra (indicated by number 4), (2) Marathawada (indicated by number 5), (3) Telangana (indicated by number 6), (4) Rayalseema (indicated by number 7) and (5) North Interior Karnataka (indicated by number 8). The Vidarbha subdivision (indicated by number 9) is drought-hit area in the monsoon season 2004. Madhya Maharashtra receives mean monsoon rainfall of 579.5 mm with high coefficient of variability (ratio of standard deviation (SD) to mean expressed as percentage) of 21.4%. All India mean monsoon rainfall is 840 mm with SD of 10% (Parthasarathy et al. 1995). Low monsoon rainfall over the Madhya Maharashtra region is due to dynamic effects of WG (Narkhedkar et al. 2015). The rainfall during the

✉ S. B. Morwal
morwal@tropmet.res.in

1 Indian Institute of Tropical Meteorology, Dr. Homi Bhabha Road, Pashan, Pune 411008, India
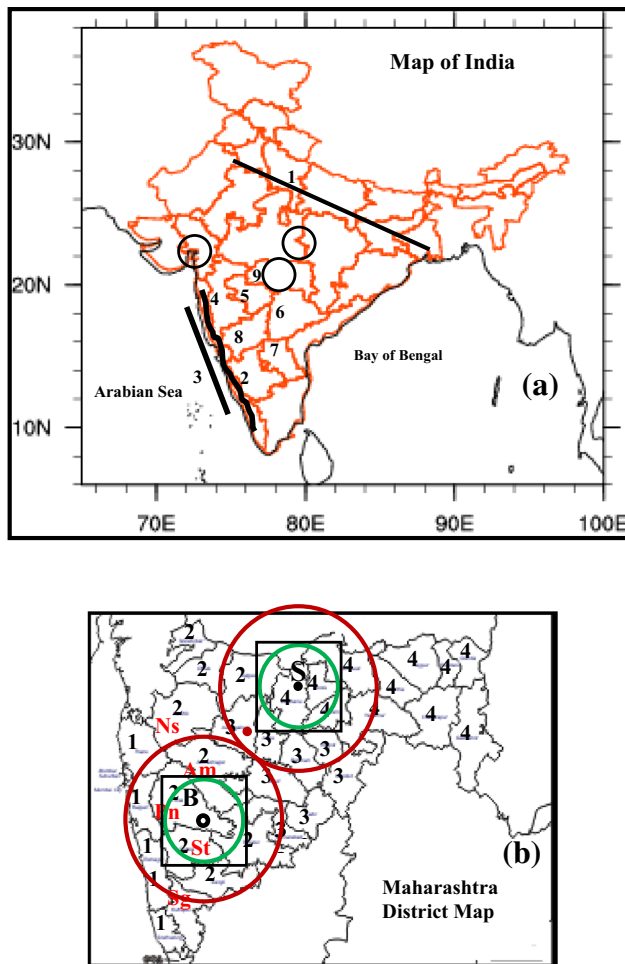
Fig. 1 a Map of India showing the cyclonic circulations (*black circles*). *Numbers 1–9* indicate: *1* monsoon trough (*straight line*), *2* Western Ghats (*zigzag line* along the west coast of India), *3* off-shore trough along the west coast of India (*straight line*). Figure shows location of the rain-shadow subdivisions Madhya Maharashtra (*4*), Marathawada (*5*), Telangana (*6*), Rayalaseema (*7*) and North Interior Karnataka (*8*) and drought-hit subdivision Vidarbha (*9*). **b** District map of Maharashtra showing: Meteorological subdivisions of Maharashtra (*1* Konkan and Goa, *2* Madhya Maharashtra, *3* Marathawada and *4* Vidarbha), radar station Baramati (B: *black open circle*), radar station Shegaon (S: *black solid circle*) along with the respective study areas (*green circles*), and the area scanned by the radars (*red circles*), study region for rainfall/ ECMWF analysis /NCEP reanalysis data (*black rectangular region*), Radiosonde station Aurangabad (*solid red circle*). Few districts of Maharashtra (*red letters Ns* Nasik, *Am* Ahmednagar, *Pn* Pune, *St* Satara and *Sg* Sangli) are also seen

summer monsoon season over these regions is widely variable (Ramachandran and Banerjee 1983; Mukherjee et al. 1979, 1980a, b).

In the past cloud seeding experiments were conducted over Madhya Maharashtra subdivision for rainfall enhancement (Murty et al. 2000). The objective of cloud seeding is to enhance the rainfall in the young, non-precipitating/ weakly precipitating convective clouds. Convective clouds

with reflectivity of 25 dBZ are in the build-up stage of rainfall initiation. Weckwerth et al. (2011) showed that convection initiates when the radar reflectivity is above the threshold of 28–36.5 dBZ. In another study, May and Ballinger (2007) showed that clouds having reflectivity of 35 dBZ are lightly precipitating. These studies indicate that convective clouds having reflectivities in the range 25–35 dBZ are in the convection initiation stage.

X and C-band radars are precipitation radars (Doviak and Zrnic 2006; Bringi and Chandrasekar 2001; Rinehart 2010). These detect clouds in which rainfall process is present. The earliest radar based cloud study over this region refers to Mani and Venkiteshwaran (1961) who used small airborne radar in the pre and post-monsoon seasons of 1953. X-band radar was used over northern India for cloud seeding operations in the past (Chatterjee et al. 1969, 1978, 1993, 1995, 1996; Chatterjee and Prakash 1986, 1989, 1990a, b; Prakash and Chatterjee 1997). X-band radar has the wavelength in the range 2.5–4.0 cm and frequency 8–12 GHz whereas C-band has the wavelength 4–8 cm and frequency 4–8 GHz. The X-band radar has lower range because of the low wavelengths (Rinehart 2010). Lower range (80–100 km) and higher attenuation of X-band radar limit the use of X-band radar for cloud seeding operations. In our previous paper (Morwal et al. 2016a, referred as M16 in the following discussions) we used C-band radar data for studying cloud characteristics and convection over the rain-shadow region during the post-monsoon season of 2011.

The State Government of Maharashtra conducted the cloud seeding operations over Madhya Maharashtra and Vidarbha subdivisions in the monsoon season 2004. Two C-band radars were operated from Baramati (B, Madhya Maharashtra subdivision) and Shegaon (S, Vidarbha subdivision) (locations are denoted by open and solid black circles in Fig. 1b) in the monsoon season. These provided unique cloud dataset in the monsoon season over Madhya Maharashtra and Vidarbha subdivisions. The first objective of the present study is to investigate the aggregate characteristics of clouds over the study areas.

C-band radars have been used to study cloud characteristics over eastern Atlantic in GATE (GARP (Global Atmospheric Research Program) Atlantic Tropical Experiment) by Houze and Cheng (1977) and over the west Pacific warm pool region in TOGA COARE (Tropical Ocean Global Atmosphere Coupled–Ocean–Atmosphere Response Experiment) by Johnson et al. (1999). The cloud characteristics investigated in the present paper are compared with those brought out in GATE and TOGA COARE experiments. The radars used in the present study are of same type to those used in GATE and TOGA COARE. However, radar operational and scan strategies are better in the present study. The GATE radar used 1200 UTC

observations only. Present study utilizes observations at all the hours of the day. In the GATE and TOGA COARE studies the time resolution for the volume scan was 10 min whereas it is 6 min in the present study.

Deep convection plays an important role in the vertical transport of mass, momentum and energy in the tropics (Riehl 1979). Understanding of the spatial and temporal variation of convection is helpful in understanding the general circulation of the atmosphere. Apart from this global perspective, at a regional level understanding of convection is important for understanding local circulation. Knowledge of space time variability of convection and clouds is important for identifying potential seeding opportunities. The clouds are the visible form of moist convection and therefore they are most suitable candidates for studying the convection. The tropical convection is categorized into different scales based on the area occupied by the clouds (Houze and Cheng 1977; Houze 1993; Johnson et al. 1999, M16). Studies regarding space–time variability of convection using radar data are lacking over the study region. Hence, the second objective of the paper is to understand the characteristics of prevailing monsoon convection using C-band radar derived cloud population data.

The study focuses on the statistical characteristics of clouds and not on the derived rainfalls. Hence rigorous radar calibrations and inter comparisons are not required (M16 and references there in). This approach has been used in many earlier studies carried over tropical oceanic and land regions (M16, Kumar et al. 2013a, b; May et al. 2012; May and Ballinger 2007; Johnson et al. 1999; Houze and Cheng 1977; Lopez 1976, 1977). There is a large inter-annual rainfall variability in the region (Rao 1976). So analysis of one season data may be considered as a limitation to the study. The monsoon season has characteristic feature of active and break conditions. The study is focused on cloud characteristics in active and break conditions. These active and break conditions have common features irrespective of the inter-annual variability (Rao 1976). This justifies use of single season radar data for getting representative statistical characteristics of clouds and convection. Studies using limited data have been carried out by May and Ballinger (2007) over Darwin, Australia. Other cloud studies using limited data have been referred in M16.

The convection is initiated in the convective clouds whose reflectivity is in the range 25–35 dBZ. Therefore, these convective clouds are considered as suitable candidates for the seeding operations. The third objective of the paper is to quantify seeding opportunities based on this range of reflectivities.

The flow of the paper is as follows. In all there are nine sections. The data utilized in the present study is described in Sect. 2. The meteorological conditions in 2004 monsoon season are given in Sect. 3. The statistical characteristics

of clouds (first objective of the paper) are discussed in Sect. 4. Convection characteristics (second objective of the study) are given in Sect. 5. Section 6 describes the statistics of seedable clouds (third objective of the study). The detailed discussion of large scale dynamical and thermodynamical processes is given in Sect. 7. The interrelationship between the observed statistical properties of clouds, convection and population of seedable clouds (three objectives of the paper) is discussed w.r.t. the large scale dynamical and thermodynamical forcing in Sect. 8. Section 9 is the concluding session.

2 Data

Two 5 cm C-band radars were operated from 23 June–30 September 2004 (study period) one each at Baramati (18.18ºN, 74.61ºE, 552 m amsl) and Shegaon (20.78ºN, 76.68ºE, 288 m amsl) as a part of the Rain Enhancement Program of the State Government of Maharashtra. Radars had a range of 250 km in the horizontal (marked by red circles in the Fig. 1b). There were 26 horizontal levels located at 0.75 km intervals in the vertical starting with first level at 1 km. Full-volume radar data at 6 min resolution was interpolated to Cartesian grids with $0.75 \text{ km} \times 0.75 \text{ km} \times 0.75 \text{ km}$ resolution. The volume consisting of $0.75 \times 0.75 \times 0.75 \text{ km}^3$ is minimum detectable volume. At a distance >120 km from the radar, the cloud detection by the radar is limited by beam spreading and minimum detectable reflectivity above the noise level (May and Ballinger 2007; Kumar et al. 2013b). Therefore, areas spanned by 120 km radius (marked by green circles in Fig. 1b) from Baramati and Shegaon have been taken for the study. These areas are referred as Baramati and Shegaon regions, respectively. Each area consisted of 264×264 grid points at the resolution of 0.75 km. The radar's technical details are given at the web-site of Weather Modification Inc. (http://www.weathermodification.com/weather-radar-systems.php). TITAN (Thunderstorm Identification, Tracking, Analysis and Nowcasting) software (Dixon and Wiener 1993) has been used to identify clouds from radar reflectivity data. TITAN software has been used for cloud characteristic studies by May and Ballinger (2007) and Kumar et al. (2013a). The radar calibrations were similar to that described in M16. The clouds are identified as 3-D regions with minimum reflectivity of 5 dBZ in the Cartesian volumes, as per the procedure followed by Kumar et al. (2013a, b), May et al. (2012), May and Ballinger (2007) and M16. Total 6797, 9469 clouds (Tables 2, 3) were observed over Baramati and Shegaon regions, respectively.

Synoptic features prevailing during 2004 over the study areas have been taken from Indian daily weather reports (Weather in India 2005). Daily gridded rainfall data at a

resolution of $1° \times 1°$ for the study period has been taken from India Meteorological Department (IMD) website (http://www.imdpune.gov.in) for the rectangular regions around Baramati (16–20ºN, 73–76ºE, black rectangle in Fig. 1b) and Shegaon (19–22ºN, 75–78ºE, black rectangle in Fig. 1b). This has been used for identifying monsoon activity over the two regions. Upper air radiosonde data of the nearest station Aurangabad (19.9ºN, 75.3ºE) (shown by red solid circle in Fig. 1b) have been downloaded, for the study period, from the website of University of Wyoming (http://weather.uwyo.edu/upperair/sounding.html) for understanding the thermodynamical structure of the atmosphere and thermodynamic forcing. In order to estimate the dynamic parameters over the Baramati and Shegaon regions gridded data have been downloaded from daily analysis of ERA Interim, Atmospheric model from European Centre for Medium-Range Weather Forecasts (ECMWF) (http://data-portal.ecmwf.int/data/d/interim_full_daily/levtype=pl) (Dee et al. 2011) at 00/12 Z. Daily mean values of ECMWF data have been computed by simple averaging of 00 and 12 Z data. The data have resolution of 0.125×0.125 latitude/longitude. Using the wind data, wind shear in the lower (850–925 hPa) and middle (400–850 hPa) layers, convergence/divergence and vertical velocity "omega" fields at 925, 850,700, 600, 500, 400, 300, 250, 200, 150 100 hPa levels have been computed. NCEP/NCAR reanalyzed latent and sensible heat flux data at $2.5° \times 2.5°$ latitude/longitude resolution (http://www.esrl.noaa.gov/psd) (Kalnay et al. 1996) have been used for computing Bowen ratio.

3 Meteorological conditions in the 2004 monsoon season

Monsoon circulation has number of stationary features at different levels. These are: (1) monsoon trough (MT) at surface (shown by 1 in Fig. 1a) (2) Mascarene high at surface, (3) westerly low level jet (LLJ) at 850 hPa level, (4) Tibetan high at 200 hPa level and (5) tropical easterly jet (TEJ) at 100 hPa level (Krishnamurty and Bhalme 1976). The monsoon circulation developed due to these stationary forcings provides moisture and convergence at lower levels to form clouds during the monsoon season. Apart from this, there are a few transient features. These are: (1) low pressure systems (LPS) over central India and Bay of Bengal (BoB), (2) off-shore west coast trough (WCT) at surface (black solid line indicated by number 3 in Fig. 1a) and (3) Cyclonic circulations in the lower (850 hPa) and middle (700–500 hPa) levels over central India (black circles in Fig. 1a). LPS are categorized into low, depression, deep depression and tropical cyclone depending on minimum pressure at the center of

the circulation (Mooley 1973). These LPS provide additional convergence of moisture in the lower levels for the formation of widespread and deep clouds. The monsoon circulation becomes active over entire India during presence of LPS. The moisture convergence occurs in the WCT region. Gentle orographic ascent over windward side of WG provides additional lifting of the moisture. This gives rise to formation of clouds over the windward side of the WG. These clouds are advected over Madhya Maharashtra study area by the low level westerly winds. The cyclonic vorticity associated with cyclonic circulations in the middle levels provides lifting of moisture in the mid tropospheric levels for the formation of clouds over Vidarbha region. The clouds are also formed over the Vidarbha study area when LPS is present over BoB and central India.

Monsoon onset occurred over the Baramati and Shegaon on 7 and 10 June, respectively (Weather in India 2005). In the year 2004, monsoon rainfalls over Madhya Maharashtra and Vidarbha were +16 and −31% of long term normal (Table 1). From Table 1 it is seen that normal rainfall during the summer monsoon season (June–September) over the windward side of the WG

Table 1 The actual rainfall, climatology of rainfall (mm) and departure of rainfall (%) for the months from June–September 2004 and for the monsoon season (June–September) 2004 over the meteorological subdivisions of Maharashtra State. Source: http://metnet.imd.gov.in/mausamdocs/35631.pdf

	Konkan and Goa (KG)	Madhya Maharashtra (MM)	Maratha-wada (M)	Vidarbha (V)
June (J)				
Actual	641	189	113	133
Normal	675	134	144	167
Departure	−5%	41%	−21%	−20%
July (J)				
Actual	894	151	218	225
Normal	1069	238	192	329
Departure	−16%	−37%	13%	−30%
August (A)				
Actual	1070	285	79	230
Normal	712	176	194	300
Departure	50%	62%	−60%	−23%
September (S)				
Actual	242	190	186	89
Normal	347	151	174	180
Departure	−30%	25%	7%	−51%
Monsoon season (June–September)				
Actual	2847	815	595	678
Normal	2802	700	704	976
Departure	2%	16%	−16%	−31%

(Konkan and Goa regions) is very high (2802 mm) as compared to the regions lying on the leeward side of the WG (~700 mm over Madhya Maharashtra and Marathawada). It increases in the east (~976 mm over Vidarbha).

The study period is divided into active (ACT) and break (BRK) periods based on daily area-mean rainfall amounts. The study is focused on long durations of ACT and BRK periods. The time series of area-mean daily rainfalls (mm) over Baramati (black solid line solid circle) and Shegaon (red solid line solid circle) regions during summer season of 2004 along with climatological area-mean daily rainfalls (solid lines with green color for Baramati and blue color for Shegaon) are shown in Fig. 2. The area-mean daily rainfalls during 2004 were above the climatological area-mean daily rainfall during 25 July–6 August (13 days) over both the regions. This is categorized as ACT period. During this period three LPS were present (23–24 July, 27 July–2 August, 2–6 August) over India (Weather in India 2005). Higher rainfall in this period was due to the presence of both stationary as well as transient features viz. LPS, WCT (Weather in India 2005). During the period MT was south of its normal position which is a typical feature in active monsoon conditions (Parasnis and Morwal 1991).

The area-mean daily rainfall during 2004 was below the climatology area-mean rainfall during 23 June–14 July (22 days) and 17 August–5 September (20 days). These are categorized as BRK1 and BRK2 periods, respectively. Transient features viz. WCT and cyclonic circulations in the lower and middle tropospheric levels were present during these periods. These systems provided dynamical forcing for the formation of clouds in BRK periods. BRK1 period occurred in the beginning of the monsoon season whereas BRK2 period occurred nearly at the end of the monsoon season 2004 when the monsoon was approaching the withdrawal phase.

4 Statistical cloud characteristics

The first objective of the paper is to investigate the aggregate characteristics of the clouds over the study region. This has been addressed in context with: diurnal variation, heights of cloud tops and the durations of clouds. These are described in the following sub-sections.

4.1 Diurnal variation

Among the different timescales, diurnal variation is particularly important. Clouds are most affected by the diurnal cycle of earth's surface heating/cooling and boundary layer moisture convergence. The diurnal variation has been studied over continental and marine regions (M16 and references there in) for understanding the nature of convection. Keenan et al. (1989) found maximum cloud frequency around 1430–2030 h local time over the land in the Australian Monsoon Experiment (AMEX). Yang and Slingo (2001) showed that deep convection over the oceanic regions tends to reach its maximum value in the early morning hours. M16 observed maximum in cloud frequency in the morning 8–10 IST (Indian Standard Time is local time which is ahead of UTC by 5 h and 30 min) and minimum in the evening 4–5 IST in the post monsoon season over the rain-shadow region.

The diurnal variations of cloud frequencies in BRK1, ACT and BRK2 periods over Baramati and Shegaon regions are shown in Fig. 3a–f, respectively. Number of clouds in BRK1, ACT and BRK2 periods are 2618, 2875, 1304 and 2694, 3811, 2964 over Baramati and Shegaon regions, respectively. These are equivalent to 119, 221, 65 clouds day^{-1} in the three periods over Baramati and 122, 293, 148 clouds day^{-1} in the three periods over Shegaon region, respectively. Maximum clouds are seen in ACT period. However, the cloud populations are not insignificant in the BRK periods but comparatively lesser in BRK2 period over Baramati. Prominent features of diurnal variability are: (1) existence of clouds all the hours of day (2) strong similarity in the frequency distributions in all the three periods. The maximum frequency is seen at 10–11 UTC and minimum at early morning hours at 3–4 UTC. The maximum frequency observed here is similar to that observed by Keenan et al. (1989), and is different from that observed by Bergman and Salby (1996) over the
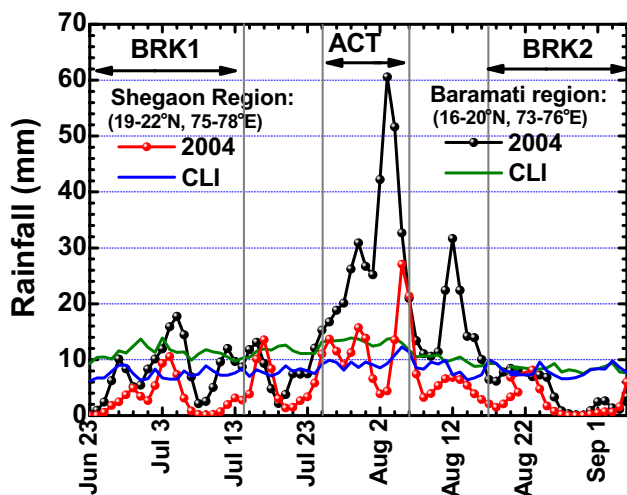

Fig. 2 Climatological (CLI: 1971 to 2005; *solid green line* for Baramati region and *blue line* for Shegaon region) and study period (2004: *black* (Baramati region) and *red* (Shegaon region) *solid lines with solid circles*) daily area-mean rainfall (mm) during 23 June–5 September over Baramati (16–20ºN, 73–76ºE) and Shegaon (19–22ºN, 75–78ºE) regions. *Vertical lines* delineate the different active (ACT: 25 July–6 August 2004) and break (BRK1: 23 June–14 July, BRK2: 17 August–5 September 2004) periods
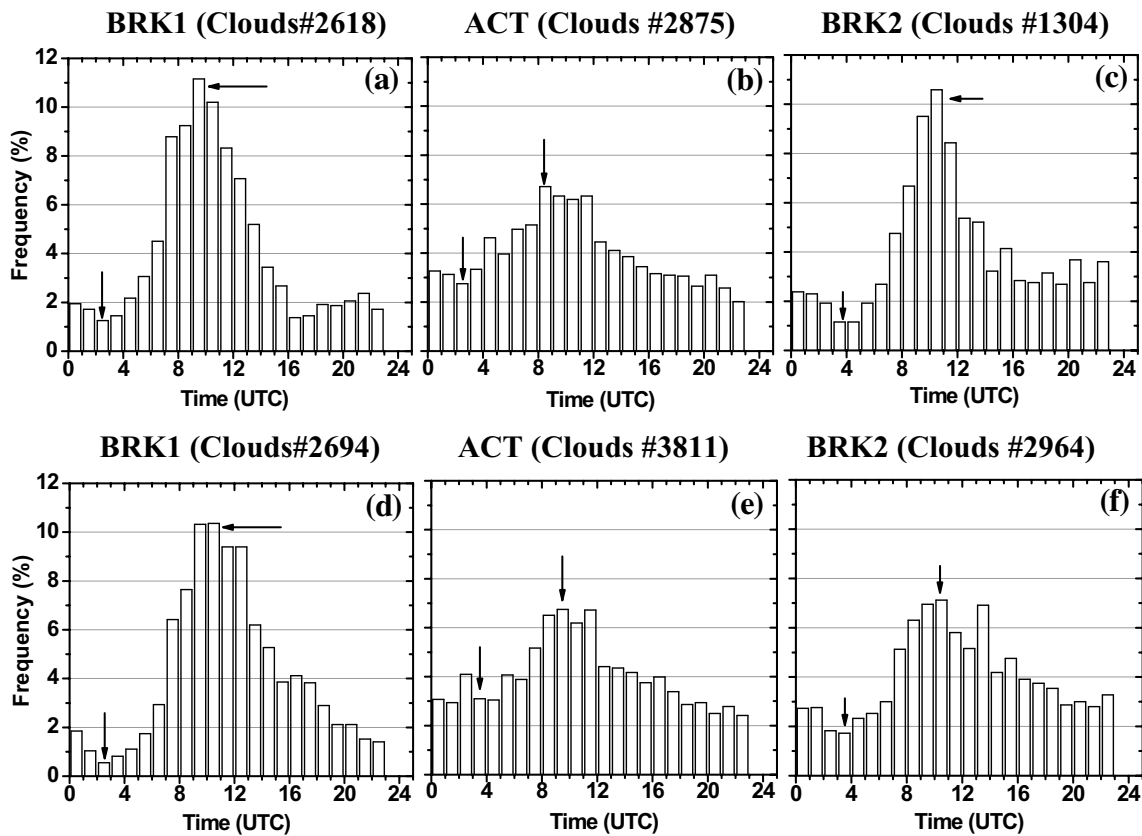
Fig. 3 Diurnal variation of number of clouds (%) over (**a–c**) Baramati and (**d–f**) Shegaon regions during break (BRK1 and BRK2) and active (ACT) monsoon conditions of 2004. *First* and *second arrows* indicate the time classes associated with the minimum and the maximum frequency, respectively

continental region and by M16 over the rain-shadow region in the post-monsoon season. The peak frequencies are 11, 7, and 11% in BRK1, ACT and BRK2 over Baramati region and 11, 7, 7% in BRK1, ACT and BRK2 periods over Shegaon region, respectively. The diurnal variation is smoother (less difference between maximum and minimum) in ACT period as compared to BRK periods.

4.2 Distribution of cloud population

Following the methodology used by Johnson et al. (1999) and that used in M16, based on maximum cloud top heights, clouds are categorized as (1) shallow cumulus (referred as cumulus): clouds with maximum top heights from 0 to <4 km, (2) congestus: clouds with maximum top heights from 4 to ≤9 km and (3) cumulonimbus: clouds with maximum top heights >9 km. Figure 4a–f shows time series plots with 12 h resolution of cumulus (black solid line), congestus (red solid line) and cumulonimbus (blue solid line) clouds, along with the percentage of cumulative frequency distribution (represented by the same color with dashed line) of clouds in the three periods over Baramati

and Shegaon regions, respectively. These are normalized with respect to total number of clouds. It is seen that frequency of cumulus (black line) is the lowest and that of congestus (red line) is the highest with intermediate frequency of cumulonimbus (blue line in Fig. 4a–f; Table 2) clouds during BRK1, ACT and BRK2 periods. From Fig. 4a it is seen that over Baramati region the frequency of cumulonimbus clouds during BRK1 period is comparable to that of congestus on many occasions indicating the high probability of thunderstorms during this period. It is also evident that frequency of occurrence of congestus clouds is very high during the ACT period over both the regions (Fig. 4b, e).

Table 2 shows the statistics of number of clouds (normalized to total clouds) in the three periods over the two regions. The frequency of cumulus varies from 5.77 to 24.46%. The frequencies are highest in BRK2 periods over the two regions (Baramati: 17.94% and Shegaon: 24.46%). The frequencies of congestus vary from 51.15 to 71.45% over the two regions. The frequencies are higher during the ACT period over the two regions (Baramati: 67.79% and Shegaon: 71.45%). A good percentage of clouds (>51%) in
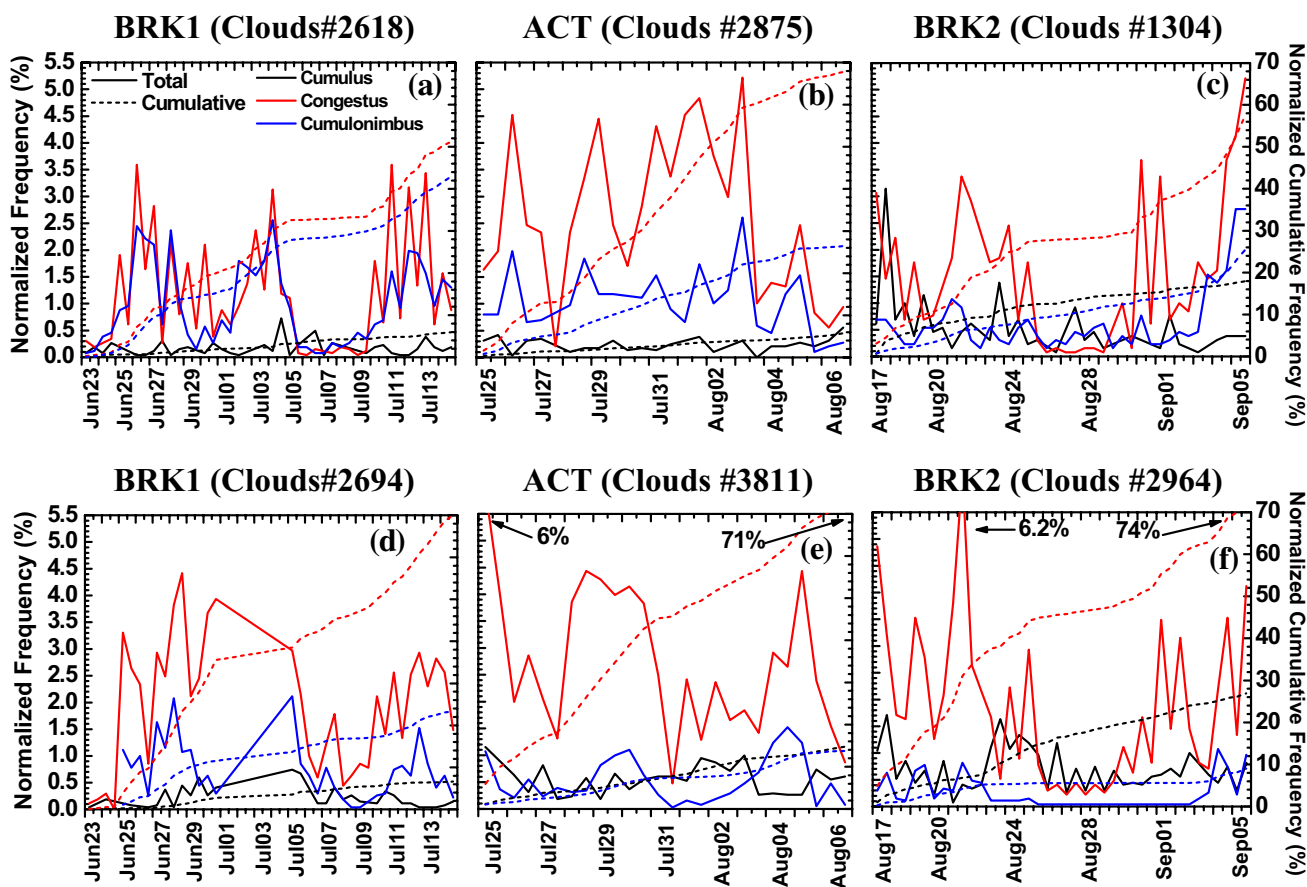
Fig. 4 12-hourly variation of normalized frequency distribution and cumulative frequency distribution for cumulus, congestus and cumulonimbus clouds (normalized w.r.t. total clouds) over (**a**–**c**) Baramati and (**d**–**f**) Shegaon regions for break (BRK1 and BRK2) and active (ACT) monsoon periods of 2004

BRK periods indicates existence of good number of opportunities for cloud seeding operations in the BRK periods. There is a large variability in cumulonimbus frequencies. It varies from 8.20 to 42.93%. The frequencies are highest in the BRK1 period over both the regions (Baramati: 42.93% and Shegaon: 23.31%).

4.3 Cloud top heights

Radar derived cloud top heights differ from actual cloud top heights. The difference is less than 1 km for deep cells and more for lower and mid tropospheric cells (Kingsmill and Wakimoto 1991; May and Ballinger 2007; Kumar et al. 2013a, M16). Even with this limitation radar derived cloud top maximum heights are found useful for understanding the broad nature of the convection and hence have been used in past studies (May and Ballinger 2007; Kumar et al. 2013a, M16). Figure 5a–f shows the frequency distributions of maximum cloud top heights over Baramati and Shegaon regions in BRK1, ACT, BRK2 periods, respectively. The vertical

grey lines delineate the three cloud categories discussed in Sect. 4.3. First four classes (1–4 km class) represent cumulus, next five classes (4–9 km) represent congestus and next 11 classes (9–19 km) represent cumulonimbus clouds. The maximum frequency in the cumulus classes is associated with the clouds having tops of 2–3 km in all the periods. In the congestus classes, the maximum frequency is in the 8–9 km class in the BRK1 and ACT periods whereas it is in the 5–6 km class in the BRK2 period. In the cumulonimbus classes, the maximum frequency is seen in the 11–12 km class in the BRK periods and in the 9–10 km class in the ACT period. The mean top maximum heights of three categories of clouds during BRK1, BRK2 and ACT periods are given in Table 2. Mean top heights are 8.93, 8.05 and 7.39 km over Baramati and 7.51, 6.74 and 5.63 km over Shegaon in BRK1, ACT and BRK2 periods, respectively. The higher mean heights in BRK1 period are due to highest frequency of cumulonimbus clouds in this period. Mean cloud top heights over both the regions are more than those observed by M16 over Telangana subdivision in the post monsoon

Table 2 Statistics of number of clouds (normalized to total clouds in %), cloud maximum top, cloud duration, cloud area (percentage contribution to the total area) for cumulus (0–4 km), congestus (4–9 km) and cumulonimbus (> 9 km) clouds for break (BRK1: 23 June–14 July and BRK2: 17 August–5 September) and active (ACT: 25 July–6 August) monsoon conditions during 2004 over the study areas of Baramati and Shegaon

Cloud type	Baramati region			Shegaon region		
	BRK1	ACT	BRK2	BRK1	ACT	BRK2
Number of clouds (normalized to total)						
Cumulus	155 (5.92%)	166 (5.77%)	234 (17.94%)	179 (6.64%)	563 (14.77%)	725 (24.46%)
Congestus	1339 (51.15%)	1949 (67.79%)	751 (57.59%)	1887 (70.04%)	2723 (71.45%)	1996 (67.34%)
Cumulonimbus	1124 (42.93%)	760 (26.43%)	319 (24.46%)	628 (23.31%)	525 (13.78%)	243 (8.20%)
Total	2618	2875	1304	2694	3811	2964
Grand total	6797			9469		
Cloud maximum top (km)						
Cumulus	2.84	2.91	2.81	2.76	3.01	2.78
Congestus	7.60	7.40	6.74	6.74	6.63	6.02
Cumulonimbus	11.35	10.82	12.29	11.20	11.30	10.88
Mean	8.93	8.05	7.39	7.51	6.74	5.63
Cloud duration (min)						
Cumulus	41.39	54.49	46.59	47.85	45.08	59.02
Congestus	37.43	40.76	44.58	42.37	52.57	59.46
Cumulonimbus	68.59	65.92	51.24	94.32	104.67	95.12
Mean	51.04	48.20	46.57	54.84	58.64	62.28
Cloud area (%)						
Cumulus	1.82	0.99	6.13	2.08	3.61	8.79
Congestus	25.06	42.81	50.42	31.76	96.39	51.66
Cumulonimbus	73.12	56.20	43.45	66.16	48.96	39.55

season (~7.67 km), that found by Braham (1958) over Tucson, Arizona semi-arid region (~6 km), that over GATE (4.8 km) (Houze and Cheng 1977) and less than those over Darwin, Australia (~8 km) during wet season (Kumar et al. 2013a).

The frequency distribution of cloud top heights in the present study is different from that observed in the GATE experiment over east Atlantic (Fig. 6 of Houze and Cheng 1977). The difference is due to absence of congestus mode over GATE region. It is also different from four cloud mode distribution over the Darwin, Australia during three wet seasons using the CPOL radar observations (Kumar et al. 2013b). First two modes observed in the present study are similar to those observed by Kumar et al. (2013b). However, the height of the congestus observed here is slightly higher than that of mode 2 observed by Kumar et al. (2013b). Mean cloud top height over the area is comparable with the heights of the 30 dBZ small convective systems over the Sulaiman Range, western foothills of Himalaya, 30 dBZ medium convective systems over the central, eastern foothills of Himalaya. However these are higher than the heights of the 30 dBZ small convective systems over the west coast of India and Myanmar (Romatschke and Houze 2011, their Table 2).

4.4 Cloud duration

The clouds are always in different stages of their life cycles. The processes of splitting and mergers are occurring at a given instant of time. At the boundary of the study area, clouds formed outside the domain enter in the study area. Similarly clouds in the study area go out of the study area. All these factors limit the accurate determination of the cloud life times. Care is taken to consider clouds which have been formed and remained in the study area in order to eliminate the clouds entering into or leaving the study area. The longer cloud durations are either due to single cloud lasting for a long period or larger cloud formed by the merging of small clouds lasting for a long period of time. These longer duration clouds lie on the extreme end of the cloud life time frequency distribution and will not affect the mean duration unless their frequencies are higher.

Figure 6a–c, g–i show the percentage frequency distribution of cloud durations during BRK1, ACT and BRK2 periods over Baramati and Shegaon regions, respectively.
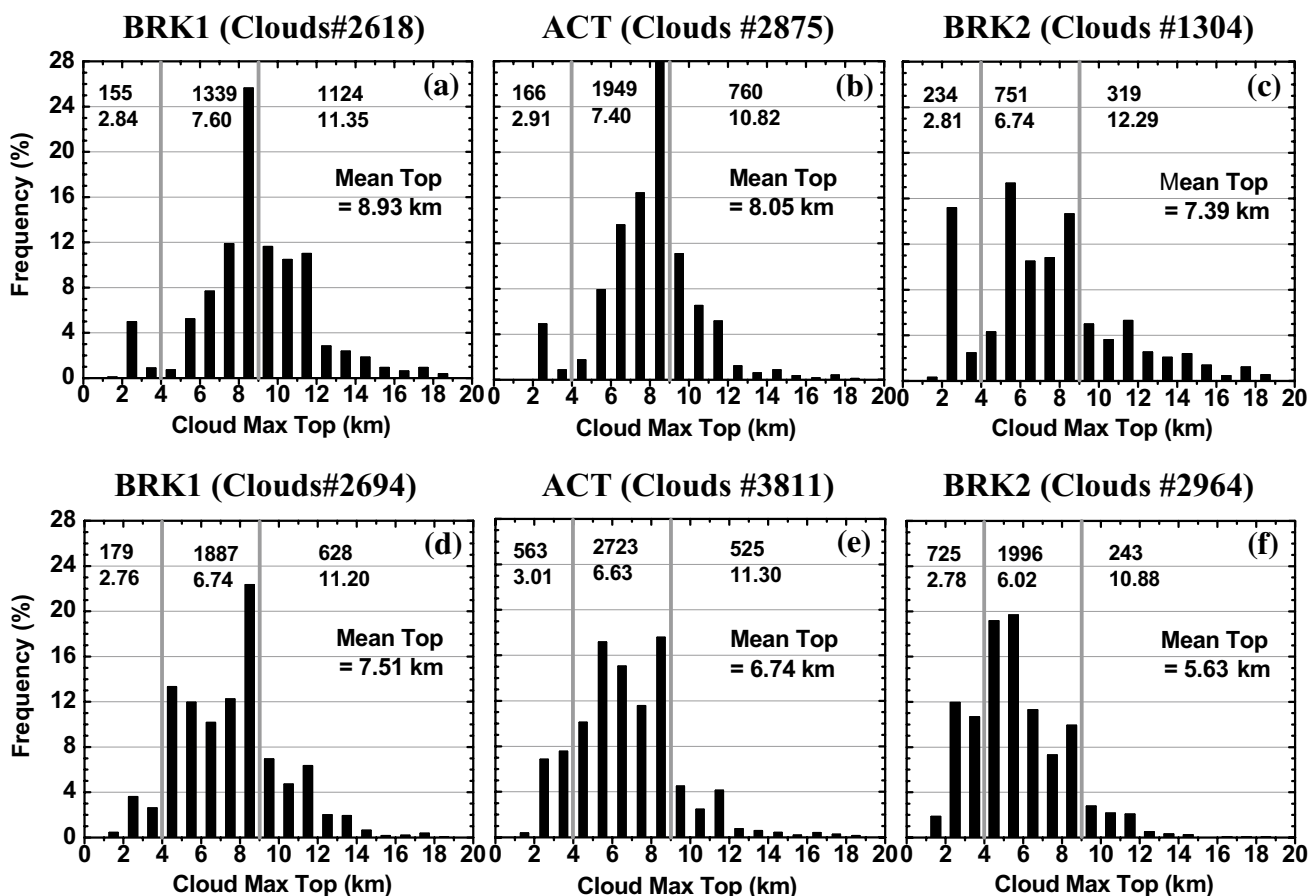
Fig. 5 Frequency distribution for cloud maximum top heights over (**a**–**c**) Baramati and (**d**–**f**) Shegaon regions during break (BRK1 and BRK2) and active (ACT) monsoon periods of 2004. The *vertical grey* *lines* represent the cumulus, congestus and cumulonimbus categories from *left* to *right*

The cloud durations are given at an interval of 25 min because the minimum cloud duration is 12 min due to availability of the volume scans at 6 min interval. However, for the convenience of presentation the plots are made at an interval of 25 min similar to that done in M16. It is seen that mean duration varies from 47 to 62 min (Table 2). The distributions are positively skewed. The first two classes contribute more (~75%) to the total cloud durations. This indicates the dominance of small duration clouds. The lowest frequencies (≤3%) are found to be associated with the longer duration clouds (duration >100 min). Therefore, the mean duration is not affected by the longer duration clouds which might have formed due to merger of smaller clouds. Intermediate frequencies (~10–13%) are linked with the medium duration clouds (50 ≤ duration ≤ 75 min). The frequency distribution is similar to that observed over eastern Atlantic in TOGA COARE (Fig. 9 of Houze and Cheng 1977). May and Ballinger (2007) observed the exponential distribution of cloud durations over Darwin, Australia. The mean duration is comparable to that observed by M16 but it is lesser than that observed over the GATE region (88 min)

(Houze and Cheng 1977) and is higher than that over the Darwin, Australia (30 min) (May and Ballinger 2007). The maximum cloud duration is 375 min. It is comparable to that observed by M16 (390 min) but lower than that reported by Houze and Cheng (1977) (500 min) over the GATE region. Thus the mean and maximum cloud durations over the study region are more or less similar to that observed by M16 in the post monsoon season, however lower than that observed over GATE area.

4.5 Testing log normality of cloud durations

The clouds are formed purely due to random process or due to dynamical forcings. The test of log normality of cloud parameters help to understand whether the variability is governed by random process or some dynamic forcing. With this point of view frequency distributions of cloud durations are tested for lognormal distribution. The lognormal distribution is associated with the parameters having a single modal value at smaller scale and progressively lower values at the larger scales (Lopez 1976;
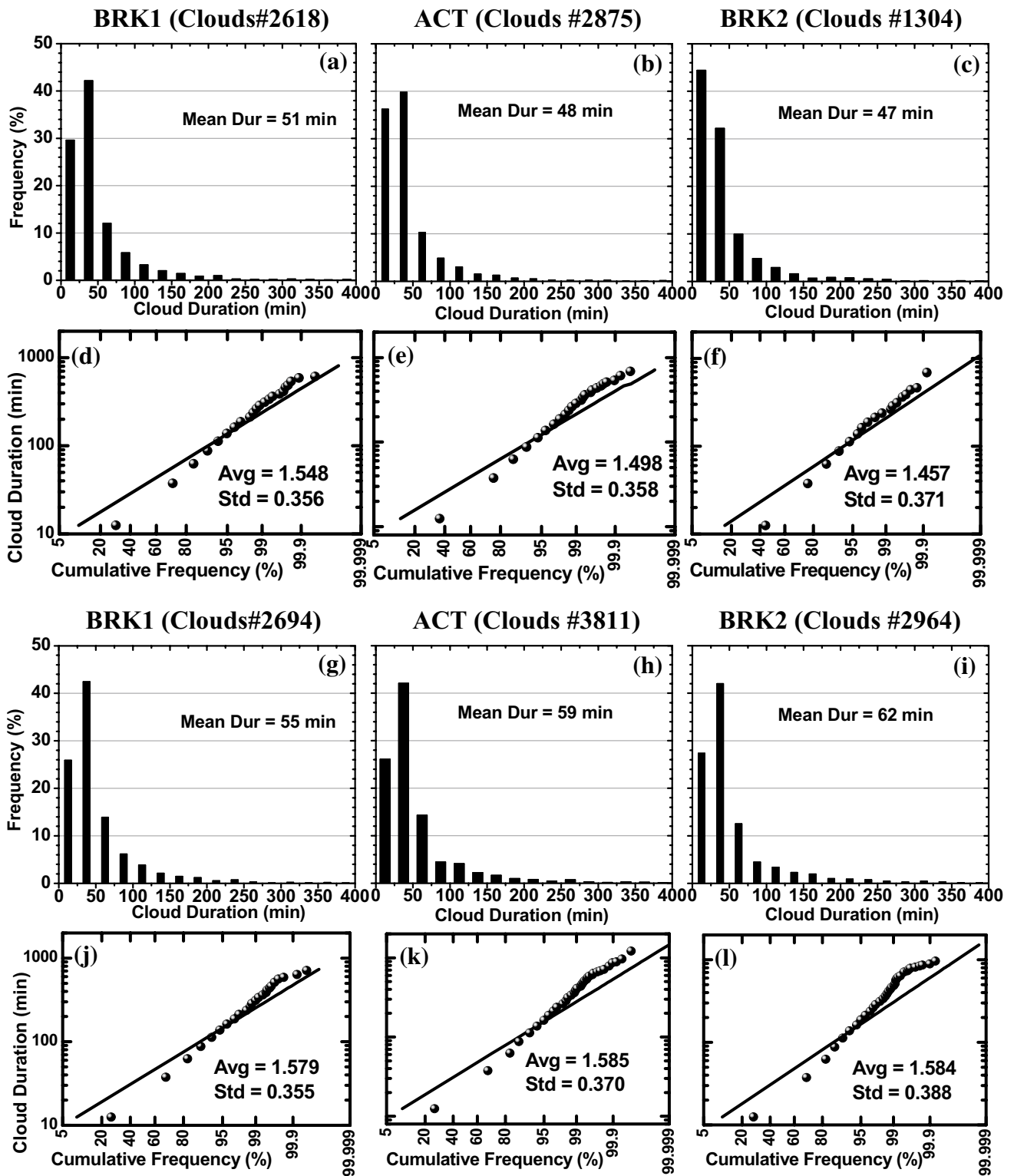
Fig. 6 Frequency and cumulative (CFD, plotted in log-probability format) frequency distribution for cloud durations over (**a–f**) Baramati and (**g–l**) Shegaon regions during break (BRK1 and BRK2) and active (ACT) monsoon periods of 2004. The *straight line* in CFD is the cumulative log-normal distribution computed from the average (Avg) and standard deviation (Std) of the logarithms of the observed cloud durations

Johnson et al. 1999). The frequency distribution of height of cloud maximum tops (Fig. 5) showed multimodal distribution and hence is not considered for testing the log normality. In Fig. 6d–f, j–l cumulative frequency distributions (%, CFD) of cloud durations are shown for the three periods over both the regions. The cumulative lognormal distribution (straight line) is fitted using the mean (Avg) and standard deviation (Std) of the logarithms of the cloud durations of the respective periods as shown in all the plots. It is seen that CFD lies along the fitted lognormal distribution straight line except at the higher end of the spectrum. This feature is also observed by Lopez (1977) over different locations (shown by him in Table 3; Fig. 5) and Houze and Cheng (1977) over Atlantic in the GATE experiment (their Fig. 10). CFD for the long lived clouds (duration >200 min) are lesser than that shown by lognormal distribution. This indicates that long period clouds might have been formed due to merging of smaller clouds associated with dynamic forcing such as wind shear and not due to random processes.

5 Characteristics of convection

The second objective of the paper is to understand the characteristics of prevailing monsoon convection using C-band radar derived cloud population data. This point is discussed in this section. In the tropical atmosphere clouds occur in wide spatial scales ranging from isolated cumulus to large cloud clusters (Gambheer and Bhat 2000; Bhat and Kumar 2015). The cloud distribution over Indian region has been studied extensively using satellite radiance data (Grossman and Garcia 1990; Laing and Fritsch 1993; Roca and Ramanathan 2000; Gambheer and Bhat 2000 and; Bhat and Kumar 2015). These studies describe cloud characteristics on larger scales. Laing and Fritsch (1993) described cloud characteristics in mesoscale convective complexes (MCC) having spatial scale more than 50,000 km^2. These MCCs were associated with LPS. Sampling interval was 3 h in the study conducted by Gambheer and Bhat (2000). Low clouds are not detected under the high cloud cover in the satellite observations. The radar gives cloud information with high spatial time resolution in the lower end of the cloud size spectrum overcoming the limitations in the satellite observations.

5.1 Scale wise cloud statistics

As was done in M16, the convection has been classified into different spatial scales based on cloud sizes. These are: synoptic scale (Scale A: size >10^6 km^2), cloud cluster scale (Scale B: size 10^5–10^6 km^2), mesoscale-1 (Scale B/C: size 10^3–10^5 km^2), mesoscale-2 (Scale C: size 10^2–10^3 km^2) and cumulus scale (Scale D: size 1–10^2 km^2). The radar observations are taken up to 120 km range, which limits identification of clouds up to B/C scales only. Figure 7a–f

Table 3 The average number of clouds (%), cloud area (%), cloud maximum top and cloud duration for D scale (area: 1–100 km^2), C scale (area: 100–1000 km^2) and B/C scale (area: 1000–10^5 km^2) for break (BRK1:23 June–14 July and BRK2: 17 August–5 September) and active (ACT: 25 July–6 August) monsoon conditions of 2004 over the study areas of Baramati and Shegaon

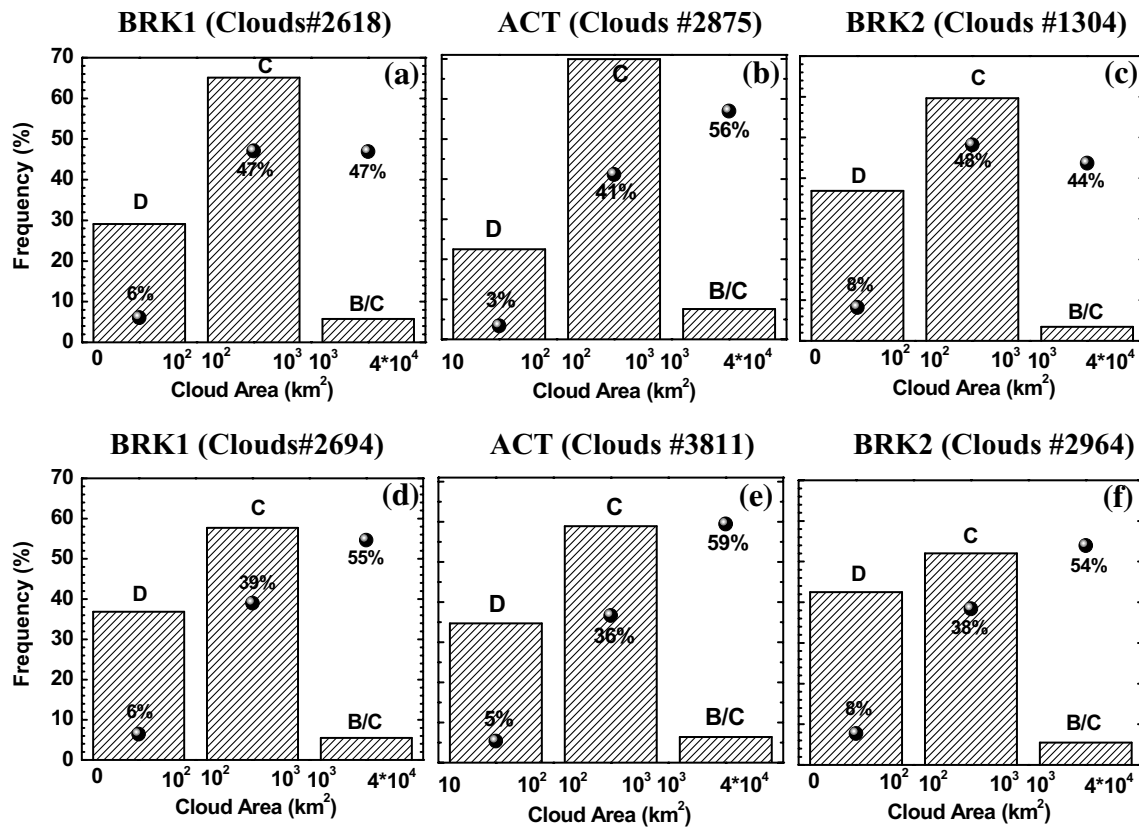| Scale type	Baramati region			Shegaon region		
	BRK1	ACT	BRK2	BRK1	ACT	BRK2
Number of clouds (%)						
D scale	29.11	22.47	36.89	36.82	34.71	42.48
C scale	65.13	69.95	59.66	57.68	58.91	52.02
B/C scale	5.77	7.58	3.45	5.49	6.38	5.50
Total	2618	2875	1304	2694	3811	2964
Grand total	6797			9469		
Cloud area (%)						
D scale	6.03	3.29	8.18	6.39	5.26	7.67
C scale	47.05	40.55	48.16	38.97	36.13	38.38
B/C scale	46.92	56.15	43.66	54.63	58.60	53.94
Cloud maximum top (km)						
D scale	7.84	7.18	6.75	5.94	5.29	4.37
C scale	9.13	8.13	7.68	8.13	7.23	6.323
B/C scale	12.10	9.85	9.23	11.56	10.14	8.80
Mean	8.93	8.05	7.39	7.51	6.74	5.63
Cloud duration (min)						
D scale	22.71	24.60	26.22	27.58	28.31	32.29
C scale	49.25	42.24	47.85	55.94	56.77	65.83
B/C scale	214.23	173.16	241.93	226.11	241.12	260.26
Mean	51.04	48.20	46.57	54.84	58.64	62.28

Fig. 7 Frequency of occurrence of radar clouds of D, C and B/C scales over (**a–c**) Baramati and (**d–f**) Shegaon regions for break (BRK1 and BRK2) and active (ACT) monsoon periods of 2004. Solid circle indicates the area occupied (%) by the clouds in each scale

shows the frequencies of occurrences of D, C and B/C scales along with the percentages of areas occupied by them (value along with big solid circle) over Baramati and Shegaon regions for the periods BRK1, ACT and BRK2, respectively. The frequencies of D scale are 29, 22 and 37% over Baramati and 37, 35 and 42% over Shegaon in BRK1, ACT and BRK2 periods, respectively (Table 3). Houze and Cheng (1977) observed that the frequencies of occurrences of D scale echoes were 72, 68 and 55% in Phase I, II and III over the GATE region during the summer season. Thus, the present values of D scale are much smaller as compared to the values over the GATE region. These are lesser than those observed by M16 in the post monsoon season. It is seen from Fig. 7a–f that the horizontal areas covered by the D scale in these periods over the two regions are 6, 3, 8% and 6, 5, 8%, respectively (Table 3).

The frequencies of occurrences of C scale clouds are 65, 70, 60% and 58, 59, 52% over Baramati and Shegaon regions in BRK1, ACT, BRK2 periods, respectively (Table 3). It is seen from Fig. 7a–f that the areas covered by C scale in these periods are 47, 41, 48% and 39, 36, 38% over the Baramati and Shegaon regions, respectively (Table 3). Corresponding C scale frequencies in Phase I, II and III over GATE area were 22, 25 and 40%, respectively.

The comparison indicates that C scale frequencies over GATE region are lower than that obtained in the present study.

Frequencies of occurrences of B/C scale are 6, 8, 3% and 5, 6, 5% over Baramati and Shegaon regions in BRK1, ACT, BRK3 periods, respectively (Table 3). These are the lowest among three scales. From Fig. 7a–f it is evident that the horizontal areas occupied by this scale are 47, 56, 44% and 55, 59, 54% over Baramati and Shegaon regions in BRK1, ACT, BRK2 periods, respectively (Table 3). It is seen that this scale occupies substantial area. It is noticed that C and B/C scales together occupy more than 90% of the total area.

Figure 8a–f show the relationships between the cloud scales and the cloud maximum top heights over the two regions. Table 3 shows scale wise cloud top heights in the three periods. It is clearly evident from the figure and the Table 3 that the cloud maximum top height increases from D to B/C scale for all the periods. The D scale heights are 7.84, 7.18, 6.75 km and 5.94, 5.29 and 4.37 km over Baramati and Shegaon regions, respectively in the three periods. The heights of D scale are lower over Shegaon region compared to Baramati region. The mean cloud top heights over the GATE region for the three scales were 4.3, 5.8 and
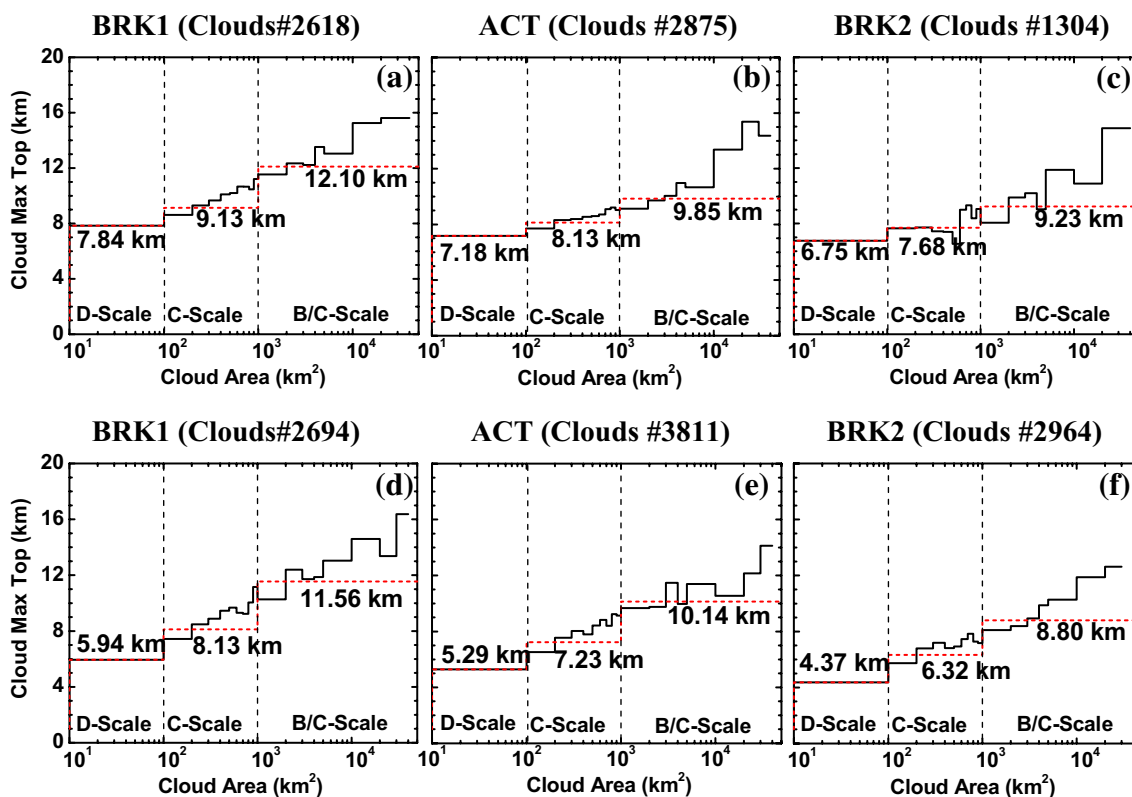
Fig. 8 Average cloud maximum top height in different size ranges (*black solid line*) and averages for different scales (D, C and B/C scales, *red dashed line*) along with its average over (**a–c**) Baramati and (**d–f**) Shegaon regions for break (BRK1 and BRK2) and active (ACT) monsoon periods of 2004

9.9 km, respectively (Houze and Cheng 1977). Thus, for D and C scales, the values over the GATE region are lower as compared to that over the study region. C scale and B/C scale clouds have higher tops in BRK1 period than in other periods. The cloud tops during the monsoon season are comparable to those observed by M16 in the post monsoon season.

The association between the cloud scales and the cloud duration during the BRK1, ACT and BRK2 periods are shown in Fig. 9a–f over the Baramati and Shegaon regions, respectively. The cloud duration was found to be positively correlated with the horizontal cloud area. Duration of D scale varies from 23 to 32 min, C scale varies from 42 to 66 min and B/C scale varies from 173 to 260 min (Table 3). Monsoon season cloud durations over the study region are smaller than those in the post monsoon season. Houze and Cheng (1977) observed that mean duration of B/C scale is more in Phase III period when there was increased synoptic scale activity.

5.2 Mesoscale convective systems (MCS) and sub-MCS

Mesoscale convective systems (MCS) are cloud clusters having large horizontal areas. Fair weather cirrus clouds

are also having a large horizontal area. However, these clouds are high in the troposphere and are not precipitating. So these are not observed by the radars. Similarly, marine stratus clouds are having a large horizontal area. Our study region is over the land and therefore marine stratus clouds are not the part of population of clouds studied here. The convection over Pacific warm pool region has been studied in TOGA COARE using MCS (Johnson et al. 1999). They divided MCS into two categories: sub-MCS and MCS. Sub-MCS category was defined if the cloud horizontal area was <100 km^2 and MCS category was defined if the area was ≥100 km^2. MCSs contain adjacent convective clouds ≥100 km^2 in scale whereas the sub-MCS category refers to clouds whose adjacent convective precipitation echoes are <100 km^2 in horizontal scale (Houze 1993). MCS have regions of both convective and stratiform precipitation (Houze 2004). These two categories represent the isolated (sub-MCS) and organized (MCS) convection. Echo height distribution plots have been used by DeMott and Rutledge (1986) for all the three cruises of the Vickers and by Lopez (1976) in the Barbados area. The present study has used the same approach for studying the convection. The frequency of cloud top heights (%) for the MCS (green line), sub-MCS (red line) and all the clouds (black line) are
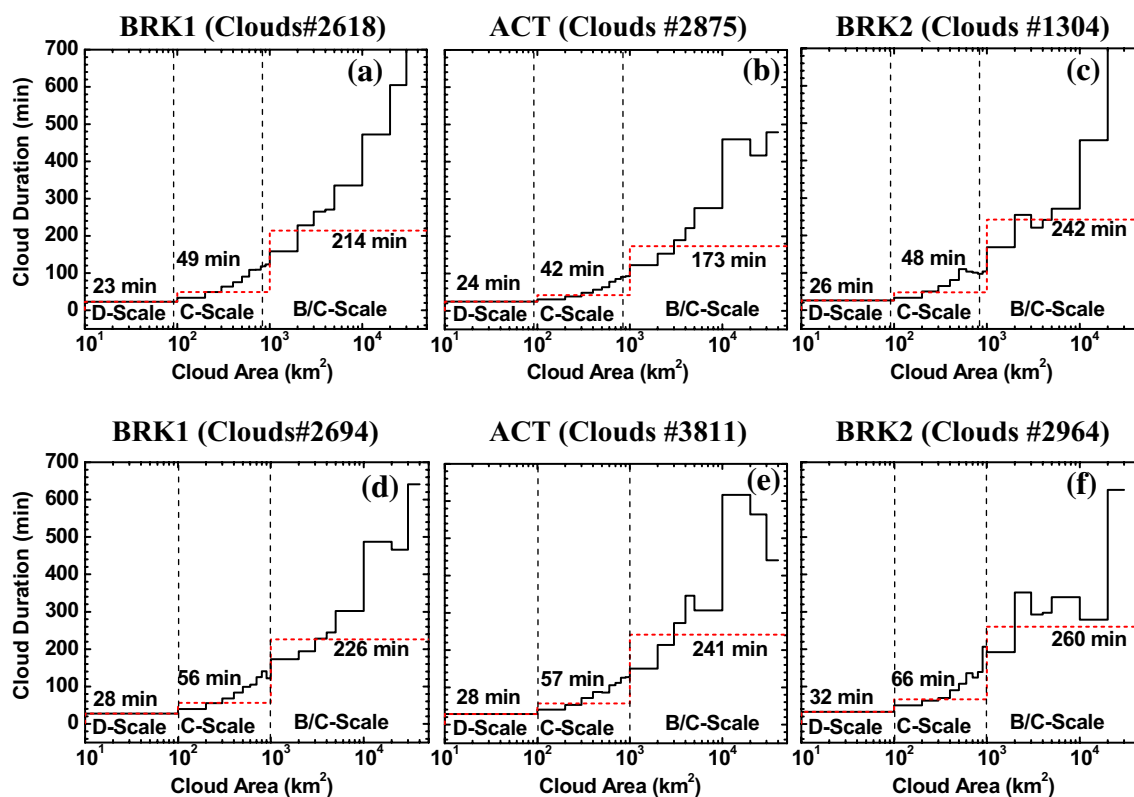
Fig. 9 Average cloud duration in different size ranges (*black solid line*) and averages for different scales (D, C and B/C scales, *red dashed line*) along with its average over (**a–c**) Baramati and (**d–f**) Shegaon regions for break (BRK1 and BRK2) and active (ACT) monsoon periods of 2004

shown in Fig. 10a–f over Baramati and Shegaon regions for BRK1, ACT and BRK2 periods, respectively. The frequency distributions are more or less similar in all the three periods. The MCS is the dominant category in all the three periods. MCS frequencies vary from 57.5 to 77.5%. Previous studies (M16, Johnson et al. 1999 and; Rickenbach and Rutledge 1998) over oceanic and land regions reported the most common occurring category as sub-MCS. It is seen that the frequency of MCS is lower in comparison to that of sub-MCS in the 2–3 km range and vice versa for heights >8 km. Johnson et al. (1999) reported sub-MCS and MCS peaks at 3.5 and 7.5 km, respectively. They concluded that the isolated (sub-MCS) convective echoes are shallower than those organized echoes (MCS). Over the study area the second mode of sub-MCS clouds is found to reach up to MCS cloud heights.

In order to understand the development of MCS it is essential to examine the vertical wind shear of horizontal winds. The vertical wind shear plays an important role in (1) organization of tropical convection (LeMone et al. 1998) and (2) interaction among the clouds to grow from small to large sizes (LeMone 1989). Many observational and numerical studies have investigated the effect of vertical wind shear on intensity and organization of MCS (Chen et al. 2015; Jensen et al. 2011; Coniglio

et al. 2006; Weisman and Rotunno 2004; Schumacher and Houze 2003; LeMone et al. 1998; LeMone 1989; Rotunno et al. 1988). Gyakum and Cai (1990) reported that vertical wind shear prevails in the lower (700–800 hPa), middle (300–700 hPa) and upper (200–300 hPa) tropospheric layers frequently. It was reported earlier that wind shear is strong if its absolute value is >4 ms^{-1} for lower layer (1000–800 hPa) and >5 ms^{-1} for middle layer (800–400 hPa) (LeMone et al. 1998). Figure 11a, b shows the time series of wind shear in the lower (850–925 hPa, solid line with open circle) and middle (400–850 hPa, solid line with solid circle) tropospheric layers over Baramati and Shegaon regions, respectively. The vertical grey lines indicate the separation of BRK1, ACT and BRK2 periods. The horizontal dashed lines mark the region of wind shear between −4 to +4 ms^{-1}. Over both the regions, it is seen that middle layer (400–850 hPa) wind shear is strong and easterly (negative) throughout the study period. Shear is stronger during the ACT period than that in BRK periods. The low layer (850–925 hPa) wind shear is westerly (positive) during majority of the study period. It is weak and oscillating about zero value in BRK1 period. It is continuously decreasing during the BRK2 period. It is strong (>4 ms^{-1}) on most of the days

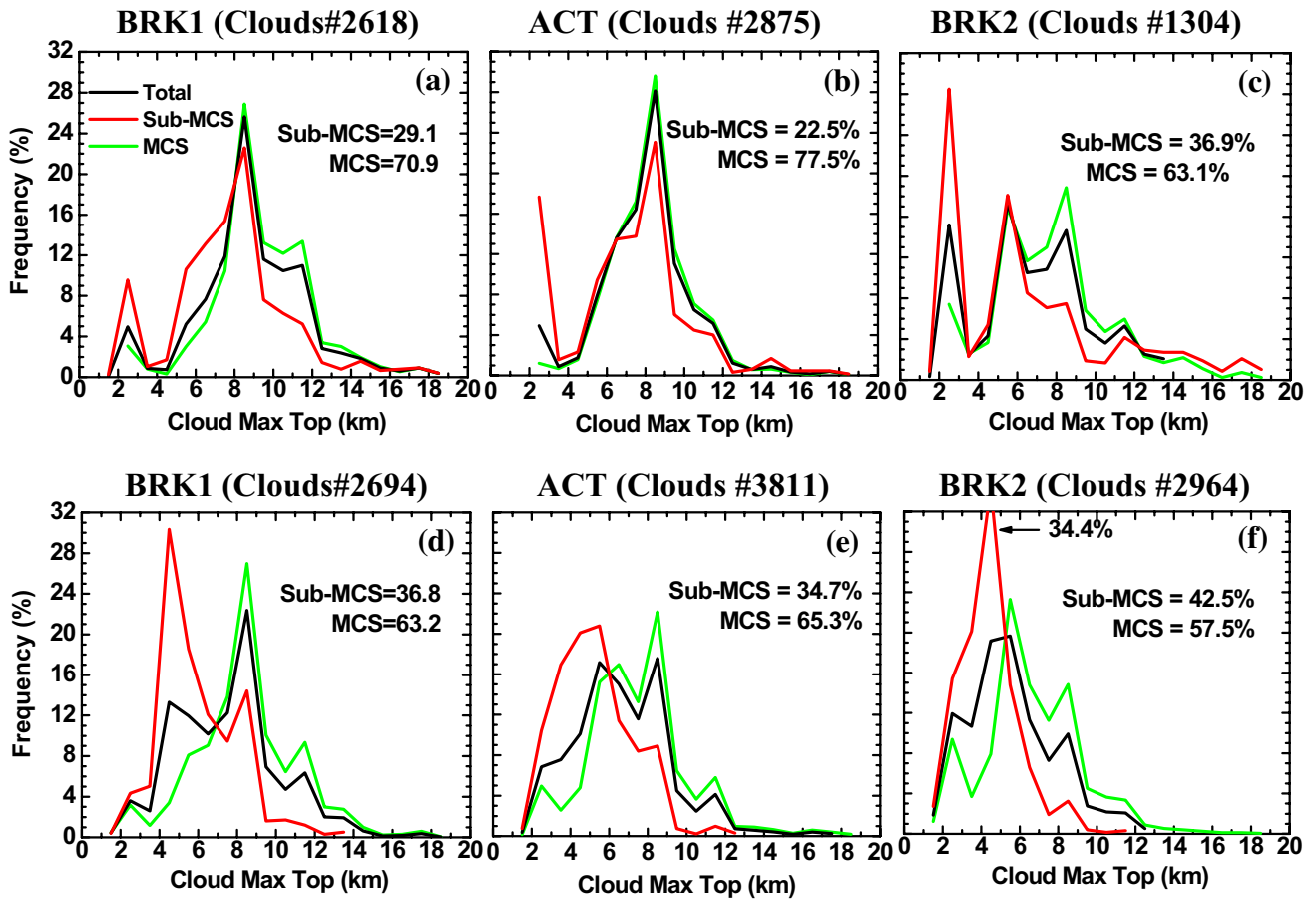**Fig. 10** Frequency distribution of cloud maximum top heights (%) of total clouds (*black line*), Mesoscale Convective Systems (MCS: *horizontal* area ≥100 km², *green line*) and sub-MCS (*horizontal* area <100 km², *red line*) categories over (**a**–**c**) Baramati and (**d**–**f**) Shegaon regions for break (BRK1 and BRK2) and active (ACT) monsoon periods of 2004
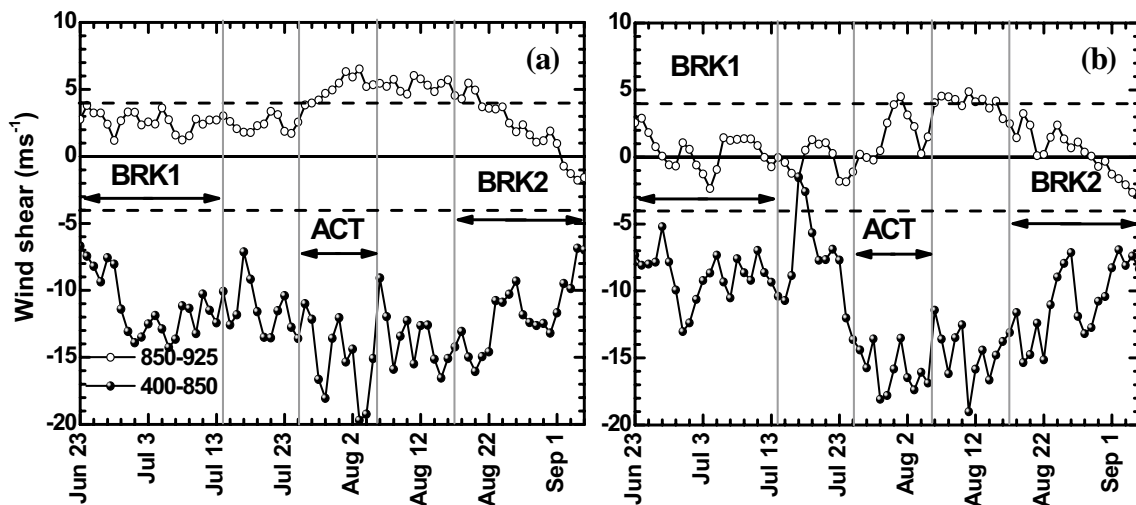

Fig. 11 Time series of wind shear (ms⁻¹) for 850–925 and 400–850 hPa layers during break (BRK1 and BRK2) and active (ACT) monsoon conditions of 2004 over **a** Baramati and **b** Shegaon regions. The *vertical lines* delineate the different monsoon conditions

during ACT period. The strong wind shears in both the layers are favorable for the organization of convection.

6 Statistics of the seedable clouds

The third objective of the paper is to quantify seeding opportunities based on the radar reflectivities. This point has been addressed in this section. The clouds are categorized into convective and stratiform based on the distribution of the reflectivity. Many schemes are available to classify the rainfall from precipitating clouds into convective and stratiform components (Churchill and Houze 1984; Steiner and Houze 1993; Rosenfeld et al. 1995; DeMott et al. 1995; Steiner et al. 1995 and; Biggerstaff and Listemma 2000). In this paper we have used the scheme of Steiner et al. (1995). In this study gridded Cartesian radar reflectivity data at 3.25 km CAPPI (Constant Altitude Plan Position Indicator) at ranges less than 120 km have been used to classify the clouds into convective and stratiform types. The algorithm has three steps as given in Steiner et al. (1995) to select the convective clouds. Any remaining nonzero reflectivity areas are then classified as stratiform.

This algorithm is applied for all the data for break and active monsoon condition over the Baramati and Shegaon regions. The frequency distribution of maximum radar reflectivity (%) for the convective (dashed line) and stratiform (solid line) clouds during break (BRK1 and BRK2) and active (ACT) monsoon conditions of 2004 over Baramati and Shegaon region are shown in Fig. 12a–f, respectively. From these plots it seen that in general the convective clouds are more as compared to stratiform clouds during both active and break monsoon conditions. During break monsoon conditions the frequency distributions of stratiform clouds showed negative skewness and leptokurtic distribution with mode around 30 dBZ (Fig. 12a, c, d, f) whereas during active monsoon conditions it is positively skewed and mode is below 25 dBZ (Fig. 12b, e). The modal value of the frequency distribution of convective clouds is more or less same and has a lesser frequency in comparison to stratiform frequency during the break monsoon conditions (Fig. 12a, c, d, f). During active monsoon conditions the modal frequencies are nearly same for the convective and stratiform clouds (Fig. 12b, e).

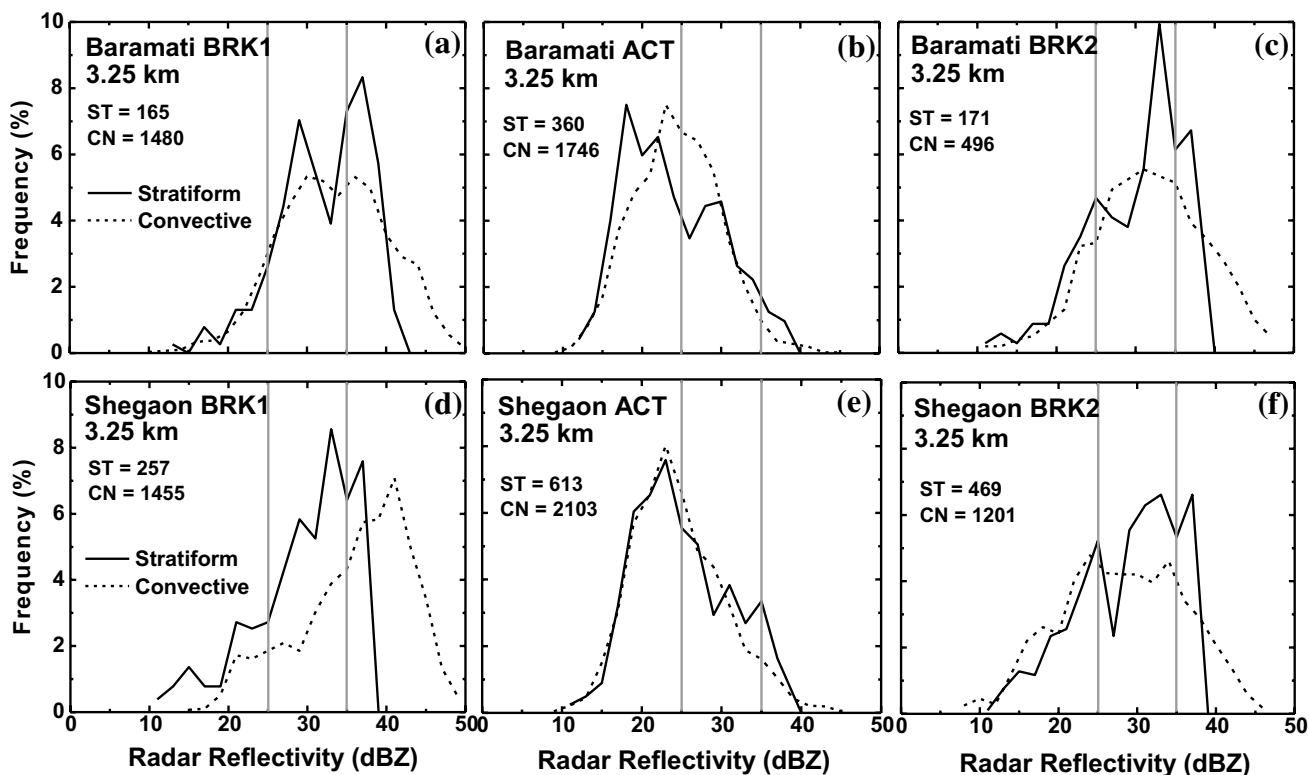The main goal of the seeding program was to increase the rainfall by hygroscopic and glaciogenic seeding. The

Fig. 12 Convective and stratiform frequency distributions for radar reflectivity at 3.25 km altitude over (**a–c**) Baramati and (**d–f**) Shegaon regions during break (BRK1 and BRK2) and active (ACT) monsoon periods of 2004. The *vertical grey lines* are drawn at 25 and 35 dBZ which is the reflectivity range for seedable convective clouds. The total number of stratiform (ST) and convective (CN) clouds are also given in each plot

experiment was conducted to enhance the precipitation as the precipitation efficiency of the clouds over this region is very low with respect to rainfall processes. Cloud seeding with large hygroscopic particles at the base and silver iodide particles in the super cooled regions of clouds is carried out to enhance the efficiency of rainfall process (Sarah et al. 2012; Murty et al. 2000; WMO 2000; Silverman 2000; Bruintjes 1999). The mean freezing level is ~5 km and the mean cloud top height in the monsoon season over study region is ~7–8 km (Fig. 5a–f). This indicates that the cloud tops are above the freezing level indicating presence of mixed-phase clouds. Hence these are suitable for glaciogenic seeding in the upper portions of the clouds where super-cooled water co-exists with ice particles. Clouds in the reflectivity range 25–35 dBZ are considered to be suitable for seeding as these are in the stage of convection initiation (May and Ballinger 2007; Weckwerth et al. 2011). Figure 13 shows the number of convective clouds with maximum reflectivities 25–35 dBZ over Baramati (red bars) and Shegaon (green bars) regions in the three periods. The number of convective clouds is the highest in ACT period. There exist a large number of convective clouds suitable for seeding even in break periods over both the regions. This indicates that good seeding opportunities are available when there is an urgent need of water for sustaining the crops. Seeding opportunities also exist in ACT periods for enhancing the existing rainfall to increase the water levels in the dams for irrigation and hydroelectric power generations. It is seen from Table 2 that the mean durations of congestus are in the range 38–60 min. These

Fig. 13 Distribution of convective clouds associated with reflectivity of 25–35 dBZ over Baramati and Shegaon regions during break (BRK1 and BRK2) and active (ACT) monsoon conditions of 2004. *Numbers in bracket* indicate the total convective clouds over the respective region. Total number of clouds in BRK1, ACT and BRK2 is also indicated

periods ensures enough time for aircraft to reach the clouds for conducting seeding operations.

7 Large scale dynamical and thermodynamical characteristics

In this section interrelationship between observed aggregate properties of clouds, convection, number of seedable clouds and large scale dynamical, thermodynamical features is discussed.

7.1 Heat fluxes and Bowen ratio

Clouds are formed because of (a) low level convergence of moist air on large scale, (b) rising of thermals due to surface heating by solar radiation (Morwal et al. 2016b) and (c) orographic lifting. The orographic lifting mechanism is absent over the study region as it is located on the leeside of WG. The thermal eddies are generated by sensible and latent heat of the Earth's surface due to solar radiation reaching the Earth's surface (Morwal et al. 2016b). The intensity of these thermal eddies govern the base and width of the convective clouds generated due to solar heating (Williams and Stanfill 2002). The Bowen Ratio (BR) is an indicator of intensity of thermals. It is defined as the ratio of sensible heat (SHF) to latent heat (LHF) flux (Bowen 1926). The time series of SHF, LHF and BR for the three periods over Baramati and Shegaon regions are shown in Fig. 14a, b, respectively. The three periods are delineated by vertical grey lines in the figure. Over the Baramati region the SHF values are in the range −10 to 30 Wm^{-2} (Fig. 14a). SHF values are relatively higher in the BRK periods and lower in the ACT periods. The LHF values range from 120 to 160 Wm^{-2}. The LHF values show oscillating feature about mean value of 140 Wm^{-2}. The BR varies from 0 to 0.13 and follows the variation of SHF. The BR values are lower in ACT periods than that during BRK periods. The low values of BR (0–0.13) during the study period indicate oceanic type of land surface (Williams and Stanfill 2002; Morwal et al. 2016b). Comparatively higher BR values in the BRK periods are conducive for intense thermals and deep clouds.

7.2 Wind divergence and vertical velocity

Figure 15a, b shows distribution of divergence (10^5 s^{-1}) and vertical velocity (Omega hPa s^{-1}) from 925 to 100 hPa levels over Baramati region and Fig. 15c, d over Shegaon region. These parameters are reported from 925 hPa because the average height of the terrain over the study region is ~500 m amsl. The three periods are delineated by black vertical lines. It is seen from Fig. 15a that
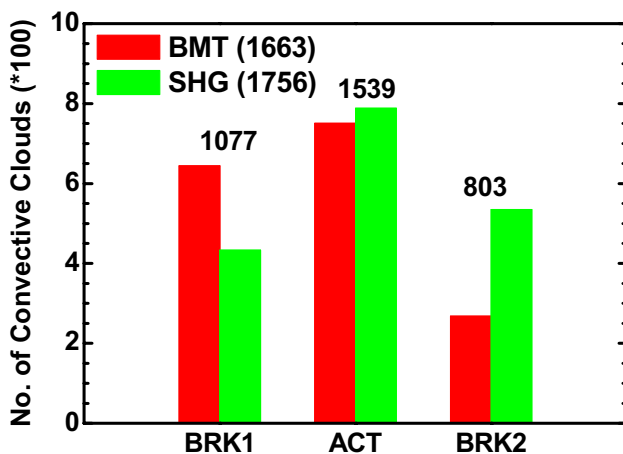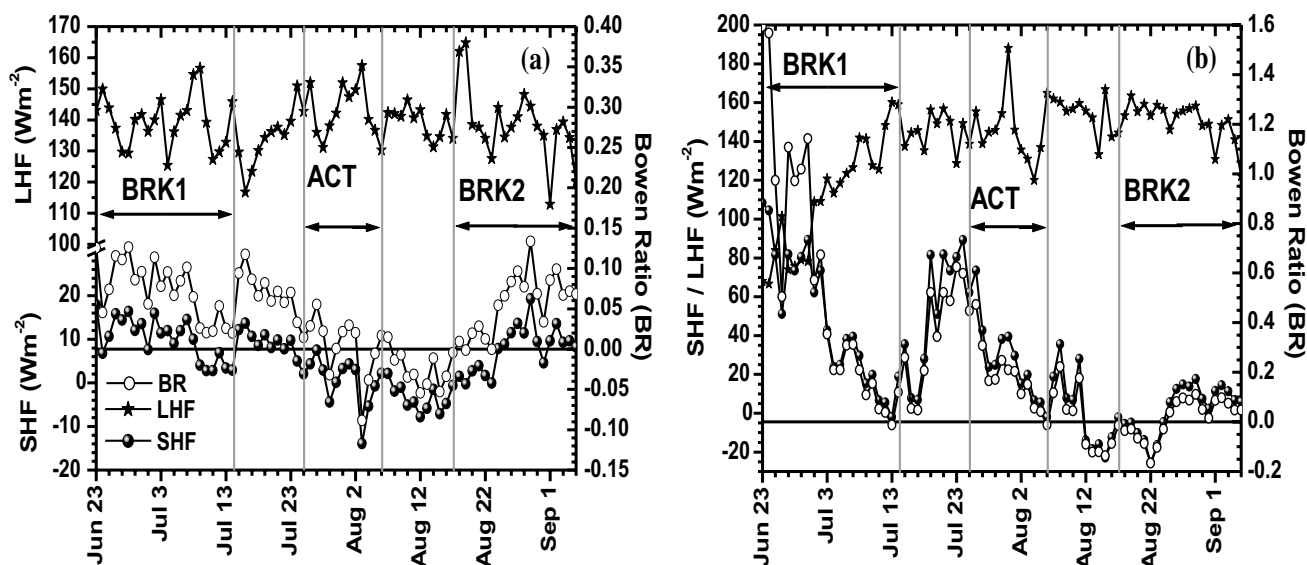
Fig. 14 Time series of latent and sensible heat fluxes (Wm^{-2}) and Bowen ratio during break (BRK1 and BRK2) and active (ACT) monsoon conditions of 2004 over **a** Baramati and **b** Shegaon regions. The *vertical lines* delineate the different monsoon conditions

over Baramati region the divergence prevails in lower (900–850 hPa) and higher (150–100 hPa) layers. The convergence is seen to prevail in the middle (850–400 hPa) layer. In the ACT period convergence is intensified. From Fig. 15c it is clearly evident that over Shegaon region the weak convergence is present in the lower levels (900–700 hPa) during the three periods. The upward motion is observed from 900 to 300 hPa level over Baramati in BRK1 period (Fig. 15b). In ACT period it extends up to 200 hPa level. Over Shegaon region, upward motion occurs above 800 hPa level (Fig. 15d).

7.3 Thermodynamical characteristics

Figure 16a shows the time series of surface thermodynamic variables viz. relative humidity (RH, %, grey line), dry-bulb temperature (Tt, °C, black line with solid circles) and dew point temperature (Td, °C, grey line with open circles) obtained from the radiosonde observations conducted at Aurangabad. The dry-bulb temperature is high~23 °C during BRK1 period and drops to ~22 °C thereafter and remains nearly constant in ACT and BRK2 periods. The dew point temperature is ~21 °C throughout the study period. Higher SHF and BR values in BRK1 period are due to higher dry bulb temperatures. The RH values are smoothed using 5 point average. High RH (>85%) is seen in all the three periods. The time series of equivalent potential temperature (θ_e, K) is shown in Fig. 16b. It is high (>340 K) on all the days. The maximum value of θ_e is 359 K. Mean value of θ_e is ~353 K in the BRK1 period and remains constant at ~349 K in ACT and BRK2

periods. Figure 16c shows the time series of CAPE (Convective Available Potential Energy, J kg^{-1}) in the study period. CAPE values are high (>1000 J kg^{-1}) in BRK1 and ACT periods. Time series of convective inhibition (CIN) is shown in Fig. 16d. Large negative values of CIN are seen in BRK1 period. In ACT periods CIN values are near to zero interspaced with moderate negative values. The time series of LCL (lifting condensation level, hPa) and LFC (level of free convection, hPa) are shown in Fig. 16e. The LFC is close to LCL on many days in all the three periods. However, there are days when LFC pressures were near to 600 hPa. The LCL and LFC are at lower levels during ACT period as compared to BRK periods by 10–12 hPa. Figure 16f shows moisture profiles in the three periods. In the ACT period RH is high (>85%) up to 400 hPa level. In BRK1 and BRK2 periods high RH is seen up 500 hPa level.

8 Discussion

As stated above, clouds are formed because of (a) low level convergence of moist air on large scale, (b) rising of moist air in thermals which are formed due to surface heating by solar radiation (Morwal et al. 2016b) and (c) orographic lifting which is non-existing over the study region. Over the rain-shadow region mechanism of rainfall has been discussed by Narkhedkar et al. (2015). Their study showed that anticyclonic vorticity and divergence are generated over the rain-shadow region below 850 hPa in the wind field due to orographic effect of WG. Further,
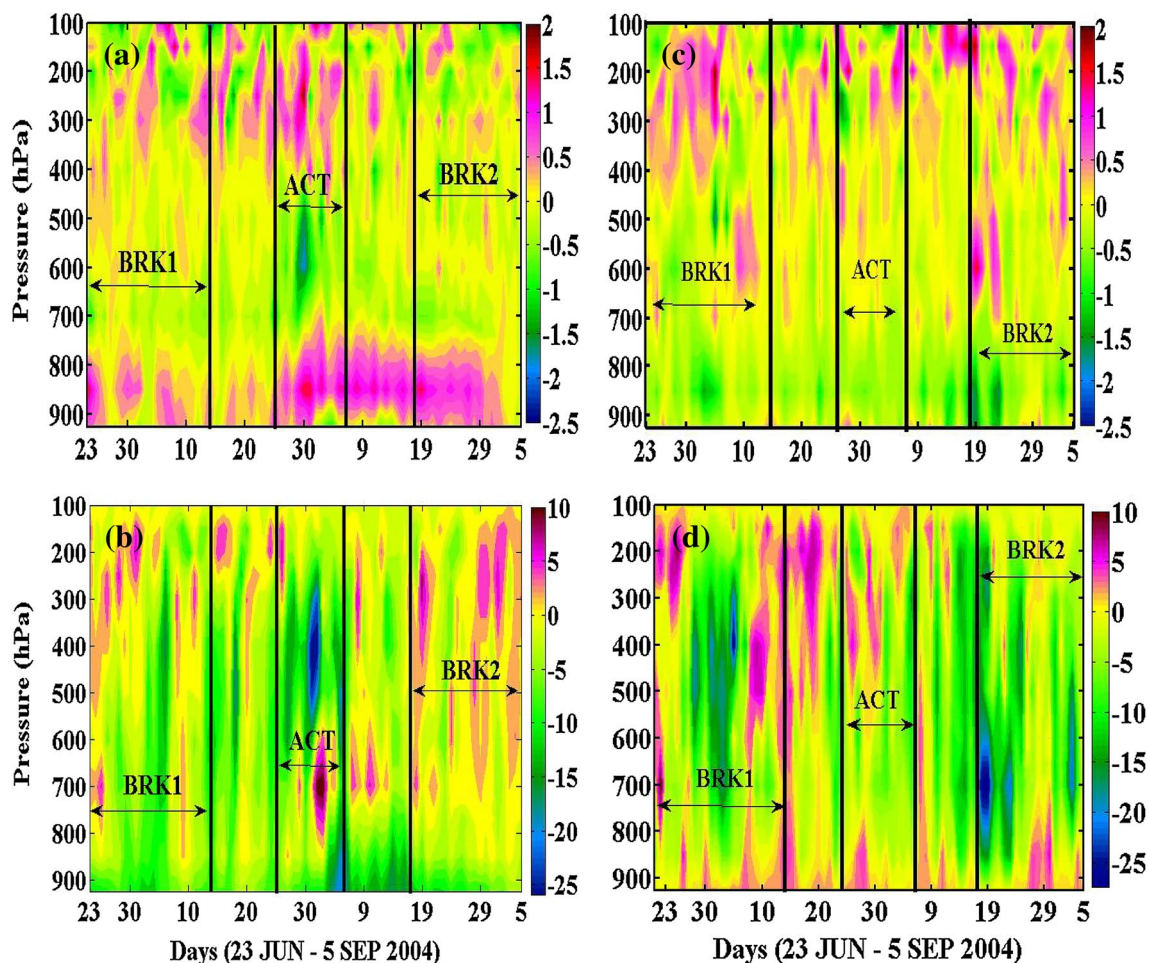
Fig. 15 Time series of divergence (10^{-5} s^{-1}) and vertical velocity (hPa s^{-1}) at standard levels of pressure during break (BRK1 and BRK2) and active (ACT) monsoon conditions of 2004 over (**a, b**) Baramati and (**c, d**) Shegaon regions. The *vertical lines* delineate the different monsoon conditions

they showed that wind convergence occurs at and above 850 hPa level which produces upward motion thereby transporting the moisture above 850 hPa level. According to Mapes and Houze (1993) convergence in the lower levels produces convection in two steps: (1) by extending the high θ$_e$ layer from the Earth's surface up to higher levels and (2) by cooling the surrounding environmental air adiabatically thereby lowering LFC of the ascending air. LFC at lower levels and close to LCL in ACT periods as seen in Fig. 16e is the result of low level convergence produced by LPS in this period.

Divergence in the low, middle and upper troposphere (Fig. 15a, c) act as a barrier by limiting the growth of convective clouds vertically and thus controls the heights of the tops of the clouds. The divergence results in producing shallow cumulus, congestus and deep convective clouds with maximum top heights at 2.5, 9 and >10 km as seen in Fig. 5.

This study showed that the BR values are low (Fig. 14a, b). Further, it is observed that these values of BR are more or less similar to the climatological values over the rain-shadow region in the post-monsoon season (Morwal et al. 2016b). Low BR values indicate ocean type surface conditions. This is because of wetness of the soil due to rainfall activity. BR values are comparatively higher in BRK periods (Fig. 14a, b) indicating generation of stronger thermals favorable for formation of deep convective clouds. The high CAPE values (especially in BRK1 period) (Fig. 16c) indicate existence of large potentials for the development of deep convective clouds. High CAPE values during BRK periods overcome the high CIN to form the clouds. It is shown in Sect. 4.3 that cloud frequencies in the classes >10 km are higher in the BRK1 and BRK2 periods than those in ACT period. Higher RH in the mid levels (seen in Fig. 16f) is due to transport of moisture by the shallow cumulus clouds which is consistent with that observed by Johnson et al. (1999) in the trade wind region.

Fig. 16 Time series of **a** surface dry-bulb (Tt, °C), dewpoint (Td, °C) temperatures and relative humidity (RH, %), **b** equivalent potential temperature (θ_e, K), **c** convective available potential energy (CAPE, kJ kg^{-1}), **d** convective inhibition (CIN, J kg^{-1}), **e** lifting condensation level (LCL, hPa) and level of free convection (LFC, hPa) and **f** vertical distribution of relative humidity (%) during break (BRK1 and BRK2) and active (ACT) monsoon conditions of 2004. The *vertical lines* delineate the different monsoon conditions
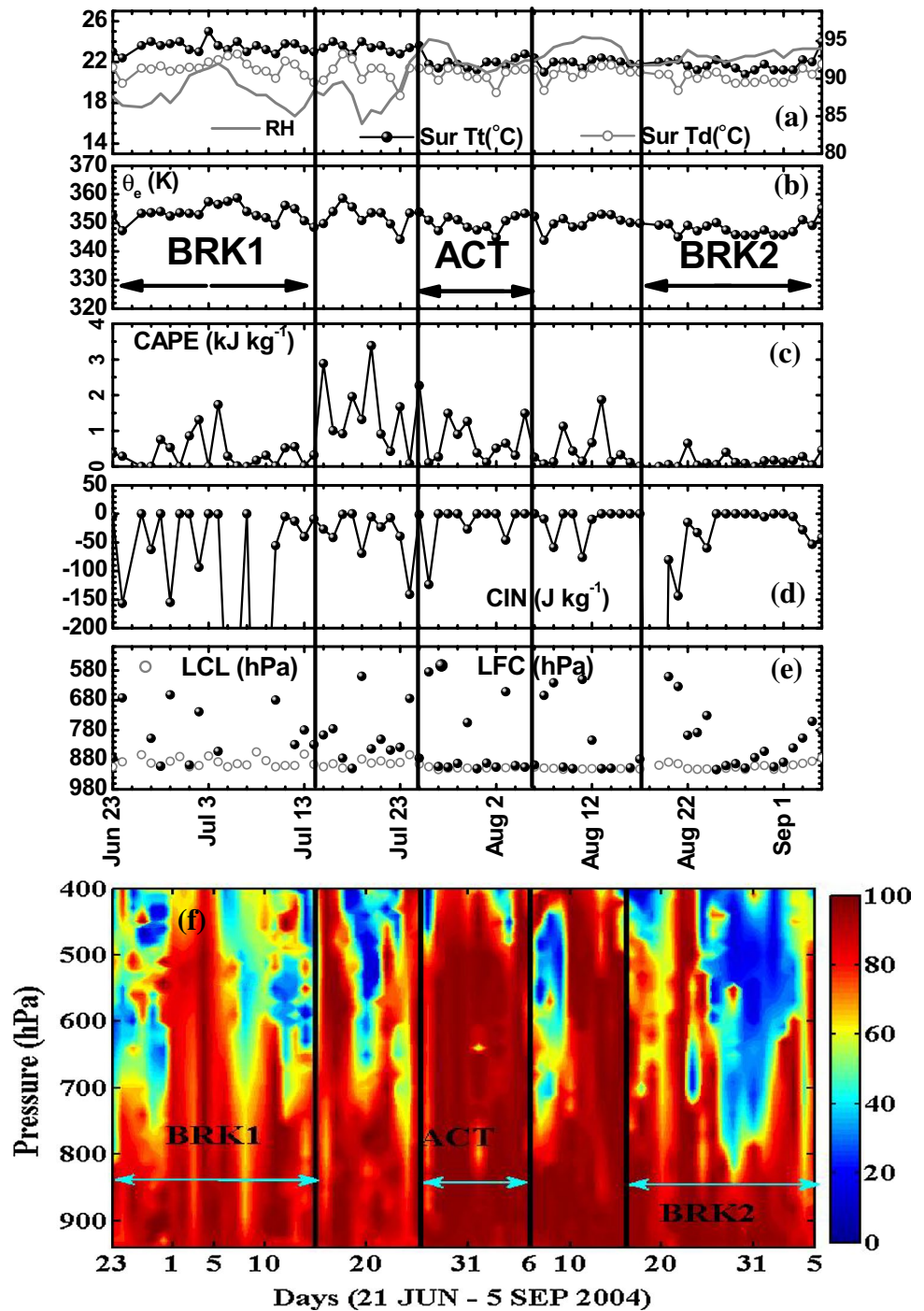
The detrainment of moisture from the tops of the shallow clouds keeps the middle troposphere moist. This middle level moisture acts as a fuel for formation of deep clouds. Thus effect of higher BR values, higher CAPE and high RH in the middle tropospheric levels in the BRK periods is to produce higher frequencies of deep clouds in BRK periods. This feature is similar to the finding of May and Ballinger (2007) that there was an increase in deep convective activity in the break conditions over Darwin.

The diurnal variation (shown in Fig. 3a–f) is smooth and is having peak in the afternoon hours at 10–11 UTC. Smooth diurnal variation indicates that convection sustains throughout the day. The surface is of oceanic type during the study period. It is well known that diurnal variation of surface temperature over the ocean is weak. Figure 16a shows that on the daily time scale, surface is warm and moist throughout the study period. This warm and moist oceanic type surface keeps the boundary layer warm and

moist over the study area to sustain the convection throughout the day producing smooth diurnal variation. Over the oceans, the diurnal variation of surface temperature is not strong. Therefore, the ocean surface remains warm throughout the night time. This warm surface provides moisture in the boundary layer. As the solar radiation heats the surface, the convection starts and clouds are formed in the morning. Whereas, over the land the diurnal cycle of surface temperature is very strong. The surface cools in the night time. The solar radiation requires a longer time to heat the surface to develop the convection currents. So the peak in the convection and clouds occur in the afternoon hours over land. The large scale convergence at lower levels is produced by stationary and transient synoptic systems throughout the day. Superimposed on this constant forcing is the thermal forcing due to land surface heating by solar radiation. Combined effect of these forcings is to shift the peak to the afternoon hours at 10–11 UTC.

The growth of clouds from D scale to C scale is due to prevailing wind shear in the lower levels resulting into maximum frequency of C scale clouds during monsoon season. This shear is also responsible for higher frequency of MCS over the study area.

Convection over the tropical rain-shadow region during the monsoon season is different from that reported earlier over other tropical oceanic and land regions (GATE, TOGA COARE and Australia). Over the GATE region frequency of D scale clouds is the highest whereas over the study region C scale is having the highest frequency. The higher C scale frequency is due to high wind shear in both lower and middle tropospheric layers during the monsoon season. The averages of maximum cloud top heights in the three scales are higher over study region than those over GATE region. Over the study region trimodal distribution of cloud types is seen whereas bimodal distribution and absence of congestus are seen over the GATE region. However, mean duration of the clouds is higher over the GATE region (88 min) than that over study region (55 min). Mean cloud duration over the study region (55 min) is more than that over Darwin, Australia (30 min). The sub-MCS category of the convection type is found dominant over TOGA COARE region whereas MCS is dominant convection type over the study region. Height of congestus is more over the study region than that over Darwin, Australia.

The differences in the convection characteristics between the study area and other tropical regions may be related to difference in surface conditions and circulation features. The surface over the study area acts like ocean (as deduced from BR values) producing oceanic type of convection. However, it is a land surface so gets some characteristics of land convection. So convection over the study area becomes hybrid type, basic oceanic type, modulated by land type. The land convection peaks in the afternoon

hours and oceanic convection peaks in the morning hours. The peak in the 10–11 UTC in the afternoon hours over the study area is in between the peaks over the land and ocean. The dominant cloud scale over the study area is C scale whereas it is D scale over the GATE area. This is due to contribution from land type convection (strong) and strong wind shear over the study area. Maximum cloud top heights of all the scales obtained in the present study are higher than those over GATE area. This feature is also due to contribution from land convection.

Monsoon circulation has stationary features like monsoon trough, Mascarene high etc. Under these stationary features, there is a slow rising motion of moist air over the Indian region which is favorable for formation of clouds. In active period the transient features like LPS are present over India. These transient features intensify the moisture convergence at low levels. This is an additional source for the formation of clouds. In break conditions, the stationary forcing is present and in addition sensible heating operates to raise the moist air for the formation of clouds. It is worthwhile to report that the convection in the two break periods over the study area is different. This feature is different from circulation features in active and break conditions over Darwin, Australia discussed by May and Ballinger (2007). Over Darwin, mean wind direction changes from westerly to easterly from active to break conditions. Over the study area wind direction remains same in both the periods as winds are driven by prevailing stationary circulation. The presence/absence of transient features leads to active/break conditions over the study area. The BRK1 occurred immediately after monsoon onset. The rainfall has just started and soil is yet to become wet completely. Low level wind shear is yet to get established. On the contrary BRK2 occurred after the ACT period. The soil has become wet. Therefore, surface temperatures and CAPE values (Fig. 16a, c) are higher in BRK1 period than those in BRK2 period. This results in higher maximum cloud top heights in BRK1 period than those in BRK2 period.

9 Conclusions

The cloud characteristics and convection characteristics over the study area have been investigated. The diurnal variation of monsoon clouds over rain-shadow and drought-hit areas showed maximum in the afternoon hours 10–11 UTC and minimum at early morning hours 3–4 UTC. The wind divergence at different levels limits the vertical growth of clouds leading to trimodal distribution of clouds viz. cumulus, congestus and cumulonimbus. The prominent cloud type over the rain-shadow region (drought-hit region) is congestus with mean heights of 7.6, 7.4 and 6.7 km (6.7, 6.6 and 6.0 km) contributing 51.2, 67.8 and

57.6% (70.0, 71.4 and 67.3%) to the total available clouds during BRK1, ACT and BRK2 periods, respectively. Mean cloud duration is 55 min with maximum duration of 375 min. The cloud duration follows lognormal distribution except at higher end. The clouds are classified based on the area covered by them into different scales from cumulus to synoptic scale. Frequency of C scale (mesoscale, $100 \text{ km}^2 \le \text{area} < 1000 \text{ km}^2$) clouds has been found maximum (52–70%). The study reveals presence of large number of convective clouds suitable for rain enhancement (reflectivity: 25–35 dBZ). The convection over the region is dominated by MCS type. The maximum cloud top heights are higher in the break periods than active period. The convection over the region is oceanic type modulated by land type. Hence, cloud characteristics are found different from those over other tropical oceanic and land regions. Understanding of the convection through cloud population will be useful in diagnostic and model studies of rainfall over the rain-shadow (drought-hit) region and for cloud seeding operations for rain enhancement.

References

Bergman JW, Salby ML (1996) Diurnal variations of cloud cover and their relationship to climatological conditions. J Clim 9:2802–2820

Bhat GS, Kumar S (2015) Vertical structure of cumulonimbus towers and intense convective clouds over the South Asian region during the summer monsoon season. J Geophys Res 120:1710–1722. doi:10.1002/2014JD022552

Biggerstaff MI, Listemma SA (2000) An improved scheme for convective/stratiform echo classification using radar reflectivity. J Appl Meteor 39:2129–2150

Bowen IS (1926) The ratio of heat losses by conduction and by evaporation from any water surface. Phys Rev 27:779–787

Braham RR Jr (1958) Cumulus cloud precipitation as revealed by radar-Arizona 1955. J Meteorol 15:75–83

Bringi VN, Chandrasekar V (2001) Polarimetric Doppler weather radar, principles and applications. Cambridge University Press, Cambridge, p 635

Bruintjes RT (1999) A review of cloud seeding experiments to enhance precipitation and some new prospects. Bull Am Meteorol Soc 80:805–820

Chatterjee RN, Prakash P (1986) Radar study of the frequency of occurrence of cumulonimbus cloud around Delhi. Mausam 37:241–244

Chatterjee RN, Prakash P (1989) Radar study of severe thunderstorm around Delhi North India during the monsoon season. Atmos Res 22:373–385

Chatterjee RN, Prakash P (1990a) Radar study of thunderstorms around Delhi during monsoon season. Mausam 41:161–165

Chatterjee RN, Prakash P (1990b) Some aspects of convective clouds around Delhi. Mausam 41:475–482

Chatterjee RN, Biswas KR, Ramanamurty BhV (1969) Result of cloud seeding experiment at Delhi as assessed by radar. Ind J Meteorol Geophys 20:11–16

Chatterjee RN, Murty ASR, Krishna K, Ramanamurty BhV (1978) Radar evaluation of the effect of salt seeding on warm maritime cumulus clouds. J Weather Mod 10:54–61

Chatterjee RN, Prakash P, Ali K (1993) Log-normal distribution of the heights of convective clouds around Delhi, North India. J Meteorol 18:161–166

Chatterjee RN, Prakash P, Singh G (1995) Frequency of thunderstorm occurrence and their height distribution in different regions in India—a radar study. Vayu Mandal 25:41046

Chatterjee RN, Ali K, Prakash P, Mujumdar SC (1996) Size distribution of radar echoes from convective clouds around Delhi during monsoon season. Ind J Radio Space Phys 25:124–128

Chen Q, Fan J, Hagos S, Gustafson WI Jr, Berg LK (2015) Roles of wind shear at different vertical levels: Cloud system organization and properties. J Geophys Res 120:6551–6574. doi:10.1002/2015JD023253

Churchill DD, Houze RA Jr (1984) Development and structure of winter monsoon cloud clusters on 10 December 1978. J Atmos Sci 41:933–960

Coniglio MC, Stensrud DJ, Wicker LJ (2006) Effects of upper-level shear on the structure and maintenance of strong quasi-linear mesoscale convective systems. J Atmos Sci 63(4):1231–1252. doi:10.1175/jas3681.1

Dee DP, Uppala SM, Simmons AJ, Berrisford P, Poli P, Kobayashi S, Andrae U, Balmaseda MA, Balsamo G, Bauer P, Bechtold P, Beljaars ACM, van de Berg L, Bidlot J, Bormann N, Delsol C, Dragani R, Fuentes M, Geer AJ, Haimberger L, Healy SB, Hersbach H, Hólm EV, Isaksen L, Kållberg P, Köhler M, Matricardi M, McNally AP, Monge-Sanz BM, Morcrette J-J, Park B-K, Peubey C, de Rosnay P, Tavolato C, Thépaut J-N and Vitart F (2011) The ERA-Interim reanalysis: configuration and performance of the data assimilation system. Q J Royal Meteorol Soc 137:553–597. doi:10.1002/qj.828

DeMott CA, Rutledge SA (1986) The vertical structure of TOGA COARE convection. Part I: RADAR echo distributions. J Atmos Sci 55:2730–2747

DeMott CA, Cifelli R, Rutledge SA (1995) An improved method for partitioning radar data into convective and stratiform components. In: Preprints 27th Conf on Radar Meteorology, Vail, CO, Amer Meteor Soc, pp 233–236

Dixon M, Wiener G (1993) TITAN: thunderstorm identification tracking, analysis and nowcasting—a radar based methodology. J Atmos Ocean Tech 10:785–796

Doviak RJ, Zrnic DS (2006) Doppler radar and weather observations. 2nd Ed, Dover Publication Inc, USA. P 562

Gambheer AV, Bhat GS (2000) Life cycle characteristics of deep cloud systems over the Indian region using *INSAT-1B* pixel data. Mon Weather Rev 128:4071–4083

Grossman RL, Garcia O (1990) The distribution of deep convection over ocean and land during the Asian summer monsoon. J Clim 3:1032–1044

Gunnell Y (1997) Relief and climate in south Asia: The influence of the western Ghats on the current climate pattern of peninsular India. Ind. J Clim 17:1169–1182

Gyakum JR, Cai M (1990) An observational study of strong vertical wind shear over North America during the 1983/84 cold season. J Appl Meteorol 29(9):902–915. doi:10.1175/1520-0450(1990)029<0902:aososv>2.0.co;2

Houze RA Jr, Cheng CP (1977) Radar characteristics of tropical convection observed during GATE: Mean properties and trends over the summer season. Mon Weather Rev 105:964–980

Houze RA Jr (1993) Cloud dynamics. Academic, San Diego, California, p 573

Houze RA Jr (2004) Mesoscale convective systems. Rev Geophys 42:1–43

Jensen EJ, Pfister L, Toon OB (2011) Impact of radiative heating, wind shear, temperature variability, and microphysical processes on the structure and evolution of thin cirrus in the tropical tropopause layer. J Geophys Res 116:D12209. doi:10.1029/2010JD015417

Johnson RH, Rickenbach TM, Rutledge SA, Ciesielski PE, Schubert WH (1999) Trimodal characteristics of topical convection. J Clim 12:2397–2417

Kalnay E, Kanamitsu M, Kistler R, Collins W, Deaven D, Gandin L, Iredell M, Saha S, White G, Woollen J, Zhu Y, Chelliah M, Ebisuzaki W, Higgins W, Janowiak J, Mo KC, Ropelewski C, Wang J, Leetmaa A, Reynolds R, Jenne R, Joseph D (1996) The NCEP/NCAR 40-year reanalysis project. Bull Am Meteorol Soc 77:437–471

Keenan TD, McBride J, Holland G, Davidson N, Gunn B (1989) Diurnal variation during the Australian Monsoon Experiment (AMEX) phase. Mon Weather Rev 117:2535–2552

Kingsmill DE, Wakimoto RM (1991) Kinematic, dynamic, and thermodynamic analysis of a weakly sheared severe thunderstorm over northern Alabama. Mon Weather Rev 119:262–297

Krishnamurty TN, Bhalme HN (1976) Oscillations of a monsoon system. Part I. Observational aspects. J Atmos Sci 33:1937–1954

Kumar VV, Protat A, May PT, Jakob C, Penide G, Kumar S, Davies L (2013a) On the effects of large-scale environment and surface types on convective cloud characteristics over Darwin, Australia. Mon Weather Rev 141:1358–1374

Kumar VV, Jakob C, Protat A, May PT, Davies L (2013b) The four cumulus cloud modes and their progression during rainfall events: A C-band polarimetric radar perspective. J Geophys Res 118:8375–8389. doi:10.1002/jgrd.50640

Laing AG, Fritsch JM (1993) Mesoscale convective complexes over the Indian monsoon region. J Clim 6:911–919

LeMone MA (1989) The influence of vertical wind shear on the diameter of cumulus clouds in CCOPE. Mon Weather Rev 117:1480–1491

LeMone MA, Zipser EJ, Trier SB (1998) The role of environmental shear and thermodynamic conditions in determining the structure and evolution of mesoscale convective system during TOGA COARE. J Atmos Sci 55:3493–3518

Lopez RE (1976) Radar characteristics of cloud populations of tropical disturbances in the northwest Atlantic. Mon Weather Rev 104:268–283

Lopez RE (1977) The lognormal distribution and cumulus cloud populations. Mon Weather Rev 105:865–872

Mani A, Venkiteshwaran SP (1961) Radar observations of thunderstorms at Poona. Ind J Meteorol Geophys 12:61–70

Mapes BE, Houze RA Jr (1993) Cloud clusters and super clusters over the oceanic warm pool. Mon Weather Rev 121:1398–1415

May PT, Ballinger A (2007) The statistical characteristics of convective cells in a monsoon regime (Darwin, Northern Australia). Mon Weather Rev 138:55–73

May PT, Long CN, Protat A (2012) The diurnal cycle of the boundary layer, convection, clouds, and surface radiation in a coastal monsoon environment (Darwin, Australia). J Clim 25:5309–5326. doi:10.1175/JCLI-D-11-00538.1

Mooley DA (1973) Some aspects of Indian monsoon depressions and the associated rainfall. Mon Weather Rev 101:271–280

Morwal SB, Narkhedkar SG, Padmakumari B, Maheskumar RS, Kothawale DR, Dani KK, Burger R, Bruintjes RT, Kulkarni JR (2016a) Cloud characteristics over the rain-shadow region of North Central peninsular India during monsoon withdrawal and post-withdrawal periods. Clim Dyn 46(1):495–514. doi:10.1007/s00382-015-2595-0

Morwal SB, Narkhedkar SG, Padmakumari B, Maheskumar RS, Deshpande CG, Kulkarni JR (2016b) Intra-seasonal and Inter-annual variability of Bowen Ratio over rain-shadow region of North peninsular India. Theor Appl Clim. doi:10.1007/s00704-016-1745-6

Mukherjee AK, Shyamala B, Mazumdar R (1979) Study of normal rainfall of Satara district. Mausam 30(4):493–500

Mukherjee AK, Shyamala B, Lakshmi L (1980a) Study of normal rainfall over central Madhya Maharashtra. Mausam 31(2):247–260

Mukherjee AK, Shyamala B, Lakshmi L (1980b) Study of rainfall over Nasik district. Mausam 31(3):397–402

Murty ASR, Selvam AM, Devara PCS, Krishna K, Chatterjee RN, Mukherjee BK, Khemani LT, Momin GA, Reddy RS, Sharma SK, Jadhav DB, Vijayakumar R, Raj PE, Manohar GK, Kandalgaonkar SS, Paul SK, Pillai AG, Kulkami CP, Parasnis SS, Londhe AL, Bhosale CS, Morwal SB, Safai PD, Pathan JM, Indira K, Naik MS, Rao PSP, Sikka P, Dani KK, Kulkami MK, Trimbake HK, Sharma PN, Kapoor RK, Tinmaker MIR (2000) 11-year warm cloud seeding experiment in Maharashtra State, India. J Wea Mod 32(1):10–20

Narkhedkar SG, Morwal SB, Padmakumari B, Deshpande CG, Kothawale DR, Maheskumar RS, Kulkarni JR (2015) Rainfall mechanism over the rain-shadow region of north peninsular India. Clim Dyn 45:1493–1512. doi:10.1007/s00382-014-2403-2

Parasnis SS, Morwal SB (1991) Convective boundary layer over the Deccan Plateau, India during summer monsoon. Bound layer Meteorol 54:59–68

Parthasarathy B, Munot AA, Kothawale DR (1995) Monthly and seasonal rainfall series for All-India homogeneous regions and meteorological subdivisions: 1971–1994. Contributions from Indian Institute of Tropical Meteorology, Research Report RR-065

Prakash P, Chatterjee RN (1997) Temporal variations of occurrence, horizontal size, height and aspect ratio of radar echoes from convective clouds around Delhi during monsoon season. Ind J Radio Space Phys 26:196–199

Ramachandran G, Banerjee AK (1983) The sub-divisional rainfall distribution across the Western Ghats during the southwest monsoon season. Mausam 34(2):179–184

Rao YP (1976) Southwest Monsoon, India Meteorological Department, Meteorological Monograph No 1/1976, p 367

Rickenbach TM, Rutledge SA (1998) Convection in TOGA COARE: Horizontal scale, morphology, and rainfall production. J Atmos Sci 55:2715–2729

Riehl H (1979) Climate and weather in the tropics. Academic, London, pp 611

Rinehart RE (2010) Radar for meteorologists. Rinehart, USA, p 482

Roca R, Ramanathan V (2000) Scale dependence of monsoonal convective systems over the Indian Ocean. J Clim 13:1286–1298

Romatschke U, Houze RA Jr (2011) Characteristics of Precipitating convective systems in the south Asian monsoon. J Hydrometeorol 12:3–25

Rosenfeld D, Amitai E, Wolff DB (1995) Classification of rain regimes by the three-dimensional properties of reflectivity fields. J Appl Meteor 34:198–211

Rotunno R, Klemp JB, Weisman ML (1988) A theory for strong, long-lived squall lines. J Atmos Sci 45(3):463–485. doi:10.1175/1520-469(1988)045<0463:atfsll>2.0.co;2

Sarah AT, Bruintjes RT, Weeks C, Wilson JW, Knight CA, Roberts RD, Peter JR, Collis S, Buseck PR, Freney E, Dixon M, Pocernich M, Ikeda K, Axisa D, Nelson E, May PT, Richter H, Piketh S, Burger RP, Wilson L, Siems ST, Manton M, Stone RC, Pepler A, Collins DR, Bringi VN, Thurai M, Turner L, McRae D (2012) The Queensland cloud seeding research program. Bull Am Meteorol Soc 93(1):75–90. doi:10.1175/BAMS-D-11-00060.1

Schumacher C, Houze RA Jr (2003) Stratiform rain in the tropics as seen by the TRMM precipitation radar. J Clim 16:1739–1756

Silverman BA (2000) An independent statistical reevaluation of the South African hygroscopic flare seeding experiment. J Appl Meteorol 39(8):1373–1378

Steiner MR, Houze RA Jr (1993) Three-dimensional validation at TRMM ground truth sites: Some early results from Darwin, Australia. Preprints, 26th Int Conf on Radar Meteorology, Norman, OK, Amer Meteor Soc, pp 417–420

Steiner MR, Houze RA Jr, Yuter SE (1995) Climatological characterization of three-dimensional storm structure from operational radar and rain gauge data. J Appl Meteorol 34:1978–2007

Weather in India (2005) Monsoon Season (June to September 2004). Mausam 56:721–756

Weckwerth TM, Wilson JW, Hagen M, Emerson TJ, Pinto JO, Rife DL, Grebe L (2011) Radar climatology of the COPS region. Q J R Meteorol Soc 137:31–41

Weisman ML, Rotunno R (2004) "A theory for strong long-lived squall lines" revisited. J Atmos Sci 61(4):361–382. doi:10.1175/1520-0469(2004)061<0361:atfsls>2.0.co;2

Williams E, Stanfill S (2002) The physical origin of the land-ocean contrast in lightning activity. C R Phys 3(10):1277–1292. doi:10.1016/S1631-0705(02)01407-X

WMO (2000) Report of the WMO International workshop on hygroscopic seeding: experimental results, physical processes, and research needs. WMP Report No 35, World Meteorological Organization, Geneva Switzerland, p 68

Xie S, Xu H, Saji NH, Wang Y, Liu WT (2006) Role of narrow mountains in large-scale organization of Asian monsoon convection. J Clim 19:3420–3429

Yang GY, Slingo J (2001) The diurnal cycle in the tropics. Mon Weather Rev 129:784–801